AN INVESTIGATION OF THE EFFECTIVENESS OF INSULATIONS IN IMPROVING CORONA CHARACTERISTICS

A Thesis

Presented to

the Faculty of Graduate Studies and Research

The University of Manitoba

In Partial Fulfillment

of the Requirements for the Degree

Master of Science

in

Electrical Engineering

---

by

A.B.M. Aminul Islam Chowdhury

October 1962

ABSTRACT

In this investigation it has been shown that corona characteristics may be greatly improved by covering a conductor with some insulation. An insulated conductor has shown even better characteristics in some respects than a bare conductor having the same overall diameter.

PREFACE

"However high we may climb in the pursuit of knowledge we shall see heights above us, and the more we extend our view the more conscious we shall be of the immensity which lies beyond."

This work is, therefore, not a complete guide to the study of corona. A great deal of study has been done on the different aspects of corona, but one field, the study of the "Effectiveness of insulations in improving corona characteristics" has had little investigation. The author has undertaken the investigation of the effectiveness of Polyvinyl Chloride and Polyethylene insulations in improving the different corona characteristics of wire conductors using co-axial cylinder arrangements.

The thesis is divided into six chapters. The first of these introduces corona and its effects and states the problem specifically. The second deals with a very short review of the laws of visual corona and discusses briefly the existing theories. The third chapter gives Schering Bridge measurements, while the fourth presents a technique of Radio Influence Voltage measurements and the results obtained therefrom. The fifth chapter explains and discusses the observed facts. In the sixth, conclusions are drawn and a comment is made

on future studies of the subject. Some lengthy developments, tables of data, and a secondary measurement technique are included in the appendices.

The author wishes to express his deep-felt gratitude to Professor G.W. Swift for his extensive help, encouragement and guidance and to Professor J.P.C. McMath for his advice and suggestions. The help received from Mr. J.R. Elliott in carrying out the experiments in the laboratory and Mrs. Flora McKechnie in typing the thesis is greatly appreciated.

Special thanks is extended to the National Research Council of Canada for its grant for the project. The author is also indebted to the Canadian Commonwealth Scholarship Committee which sponsored the scholarship and provided him with an opportunity to work on this thesis.

TABLE OF CONTENTS

TABLE OF CONTENTS CONT'D

TABLE OF FIGURES

TABLE OF GRAPHS

CHAPTER I

INTRODUCTION

1.1 CORONA AND ITS EFFECTS

For electrode configurations producing a nonuniform field, there is a certain gap length above which the gas near the surface or surfaces of maximum stress breaks down at a voltage less than the spark-breakdown voltage for that gap length. The electrical discharge at atmospheric pressure from this local breakdown is usually referred to as corona.

Positive corona on a conductor appears as a uniform bluish-white covering over the whole conductor surface; negative corona on a conductor appears as concentrated reddish tufts of glowing gas at points along the conductor. The direct current corona on the positive conductor has exactly the same appearance as the alternating current corona on the positive half of the voltage wave. The same holds for the negative conductor.[1,2*]

The electric field at the conductor surface depends on its radius, the geometry with respect to other conductors and grounded objects, and the surface condition, as well as the voltage. Since the stress

* Superscripts 1,2, etc. refer to bibliography.

is highest at the surface, the glow first starts there. Near the conductor surface the ionized air is conducting and hence the effective conductor size is somewhat increased. For the given voltage this envelope increases in thickness until the stress falls below the rupturing gradient.[2]

Corona may be undesirable due to:

1. Power Loss - The corona on a high voltage transmission line represents a continuous power loss. The causes of power loss are many. Ion collisions producing excitation and ionization of the gas atoms and molecules and increasing the thermal energy of the gas, radiation of energy from the corona envelope, various atomic processes taking place on the conductor surface and its surroundings, production of sound and light - all add to the power loss. The corona power loss on a long transmission line may be high (as great as the resistance loss[1]) and should normally be kept as low as possible. Under normal weather conditions it is usually not desirable to operate a transmission line above its critical disruptive voltage.
2. Radio Interference - Radio frequency energy is generated on a conductor when the gradient on its surface exceeds the critical disruptive value for the surrounding air. The radiation characteristics of the line, the frequency being received, as well as the r-f energy gene-

rated will determine the resulting radio interference field.[31] The pulse nature of the discharges from point corona has been studied by several investigators. According to Trichel the frequency of the pulses of negative point corona increases as the applied voltage is raised.[19] Trichel also made the first measurements of the pulses present in positive point corona.[20] According to Miller and Loeb two types of pulses are present in positive point corona and these are known as streamer and burst pulses.[23] The presence of the above pulses in the corona discharges is the major cause of radio interference. With streamer pulses the radio interference is very serious. The geometry of the system, surface conditions of discharge sources and the line voltage determine whether positive, negative or both types of pulses are present in the corona discharge.[17] Analysis of the frequency spectrum of the pulses shows that it contains appreciable components of all frequencies up to about 25 megacycles per second.

3. Insulation Deterioration[2] - Various chemical processes take place in the corona envelope. Ion bombardment and the action of certain chemical compounds that are formed due to corona cause a deterioration of insu-

lation materials. Corona is accompanied by the characteristic odor of ozone. The oxygen molecule present in the overstressed air splits into chemically very active nascent oxygen (O). These oxygen atoms may combine to form the normal molecule (O_2) or ozone (O_3). Nascent oxygen (O) readily combines with metal, organic matter etc. The unstable ozone molecule (O_3) breaks up into O_2 and O. The newly formed nascent oxygen from O_3 can readily combine with metal and organic substances. Oxides of nitrogen are also formed by the interaction of nitrogen and oxygen at very high electric stress. In the presence of moisture nitric acid may sometimes be formed.

1.2 THE PROBLEM

It was the purpose of this investigation:-

1. To measure by a Schering Bridge the power factors of a number of p.v.c. (polyvinyl chloride) insulated and bare conductors and compare the Power Factor Characteristics as a function of voltage.
2. To compare the Power Loss Characteristics as calculated from the above measurements.
3. To compare the Visual Corona Characteristics (Critical Voltage and Gradient) of bare and p.v.c. covered conduc-

tors as a function of their increase in radius over that of #14 AWG wire.

4. To compare Power Factor Characteristics of bare, p.v.c. and polyethylene insulated conductors, all having the same conductor radius, the insulation thicknesses for the insulated conductors being equal.

5. To measure the Radio Influence Voltages of p.v.c. insulated and bare conductors as a function of applied voltage.

6. To compare the Radio Noise Inception Voltage and Gradient Characteristics of both types of conductors.

7. To compare the Radio Influence Voltage Characteristics as a function of gradient.

8. To explain and discuss the observed facts.

CHAPTER II

REVIEW OF THE LITERATURE

2.1 VISUAL CRITICAL CORONA GRADIENT

The electric gradient at the surface of a conductor necessary to produce visual a.c. corona in air is given for co-axial cylinders by the empirical equation[3]

$$E_o = 30.5 m \delta \left(1 + \frac{0.305}{\sqrt{\delta r}}\right) \quad \ldots\ldots\ldots\ldots\ldots\ldots (2.1)$$

where,

E_o = Gradient at wire surface in KVP*/cm.

r = Radius of wire in cm.

m = Irregularity Factor

δ = Relative Air Density Factor and

$$= \frac{3.92b}{273 + t} \quad \ldots\ldots\ldots\ldots\ldots\ldots\ldots\ldots (2.2)$$

In equation (2.2), b is the barometric pressure in cm. of Hg. and t is the temperature in ^{0}C.

Different experimenters give different values of the constants of equation (2.1) e.g. Peek gives:

$$E_o = 31 m \delta \left(1 + \frac{0.308}{\sqrt{\delta r}}\right) \quad \ldots\ldots\ldots\ldots\ldots\ldots (2.3)$$

while others give lower values for the constants. In

* KVP = Kilovolts Peak

formula (2.1) more or less mean values of the constants are used.[3]

Investigations have shown that the gradient equation holds to a pressure of a few cm. of Hg.[1] For polished conductors the start of visual corona is quite sharp, hence the irregularity factor m is unity. For stranded conductors it varies widely and corona first starts at points of high stress and ultimately covers the whole surface. Snow, sleet, grease, oil, dust and moisture lower the corona starting gradient. Corona on a transmission line is strongly influenced by fog and rainfall and also the altitude of the line.

Equation (2.3) holds for a.c. corona. At the critical disruptive voltage the peak of the voltage wave establishes a gradient on the conductor surface dictated by this equation and corona then appears. On d.c. visual corona voltage differs slightly for conductors at positive and negative voltage. This holds equally for the positive and negative half cycles of an alternating voltage wave. In H_2, CO_2 and N_2 positive corona first starts at higher gradients than negative corona.[1] In He, O_2 and air, at pressures greater than 1 cm. of Hg, the critical gradient for positive corona is lower than that for negative corona. At pressures lower than 1 cm. of Hg, the reverse is true. For a.c. the corona voltage

is possibly determined by the first appearance of the negative discharge. This is because this discharge can reinforce the causes of positive corona in the next half cycle, thereby increasing the corona volume considerably with a corresponding increase in visibility.[1]

2.2 VISUAL CRITICAL VOLTAGE

For a co-axial cylinder arrangement the relation between the stress at the surface of the conductor and the voltage between the conductor and the outer cylinder may be used with the critical gradient from equation (2.1) or (2.3) to obtain the critical visual corona voltage. The result is:

$$V_c = E_c r \ln(R/r) \quad \text{KVP} \ldots\ldots\ldots\ldots\ldots\ldots (2.4)$$

where, R = Outer cylinder radius in cm.

2.3 PEEK'S THEORY OF VISUAL CORONA[3]

According to Peek, discharging in a gas does not necessarily occur even if the electric field exceeds the "breakdown strength" of the gas. Depending on the curvature of the electrode, the stress must exceed the breakdown strength of the gas up to a certain distance. This distance is called the "energy distance" or "storage length". Here the charge carriers gain energy to continue the discharge. The energy distance

determines the thickness of the film of ionization surrounding the electrode. Its presence permits the development of sufficient ionic energy. The energy distance is $0.3\sqrt{r}$ for the symmetrical field of a conductor inside a co-axial cylinder. For other fields similar relations with slightly different numerical values for the constants hold. Peek considers the conducting ionized gas surrounding the wire as an increase in the wire size, the whole being the "equivalent coronal conductor".

2.4 EXPLANATION OF CORONA FROM TOWNSEND'S THEORY[3]

In his theory Townsend compares corona with sparking. He makes these assumptions - (1) that cumulative ionization occurs from the corona forming conductor to the place where the electric field becomes equal to the minimum breakdown strength of the gas; and (2) that a spark discharge takes place between the conductor surface and the surface so defined. If, now, the experimental spark laws are applied to the quantities so determined, equations practically identical with Peek's equations are obtained. (This development is continued in appendix II).

2.5 MECHANISM OF CORONA FROM AVALANCHE IONIZATION

Peek's and Townsend's theories are not quite sufficient to explain all the observed facts of corona. In particular they cannot satisfactorily explain the difference in the voltage required to produce corona about positive and negative conductors. Nowadays the mechanism of corona formation is generally explained from "avalanche" ionization taking into account the effect of space charges formed therein.

High energy cosmic, ultraviolet and x-rays, natural radioactivity and other ionizing radiations always produce free electrons in the atmosphere. These electrons are closely related to the formation of corona. Of course, under certain conditions, electrons may also come from the electrode itself. However, when a voltage between two electrodes is applied the electrons are drifted toward the positive electrode. With a sufficiently high voltage the accelerated electrons gain energy to cause ionization by collision and produce space charges. For positive and negative electrode potentials the production of space charges and their motion, as well as the other processes taking place on and near the electrode surface differ widely. So, it is quite reasonable to have a difference in their corona characteristics.

For the co-axial cylinder arrangement, the action of the space charges formed with alternating current as described by J.D. Cobine,[1] is shown in figure (2.1) for somewhat idealized conditions. In this figure sharply defined boundaries are shown for the space charges, though actually they would have diffuse boundaries. He considers corona has already occurred and explains the cycle as follows:

At an instant (A), when the applied voltage is zero, a residual negative space charge exists between the cylinders due to the previous half cycle of negative corona. At this instant, lines of force start from positive bound charges on both wire and cylinder and terminate at the negative space charge. There is, therefore, a field at both surfaces even though the voltage between the surfaces is zero. As the voltage increases, additional positive bound charges appear at the conductor surface, the positive bound charges on the cylinder decrease and the space charge moves inward. Ionization by collision and the initiation of positive corona occur at an instant (B), when the field at the conductor surface is sufficiently high. (If the voltage is greatly in excess of the critical corona voltage, the residual space charge may produce a field at the conductor surface which is sufficient to

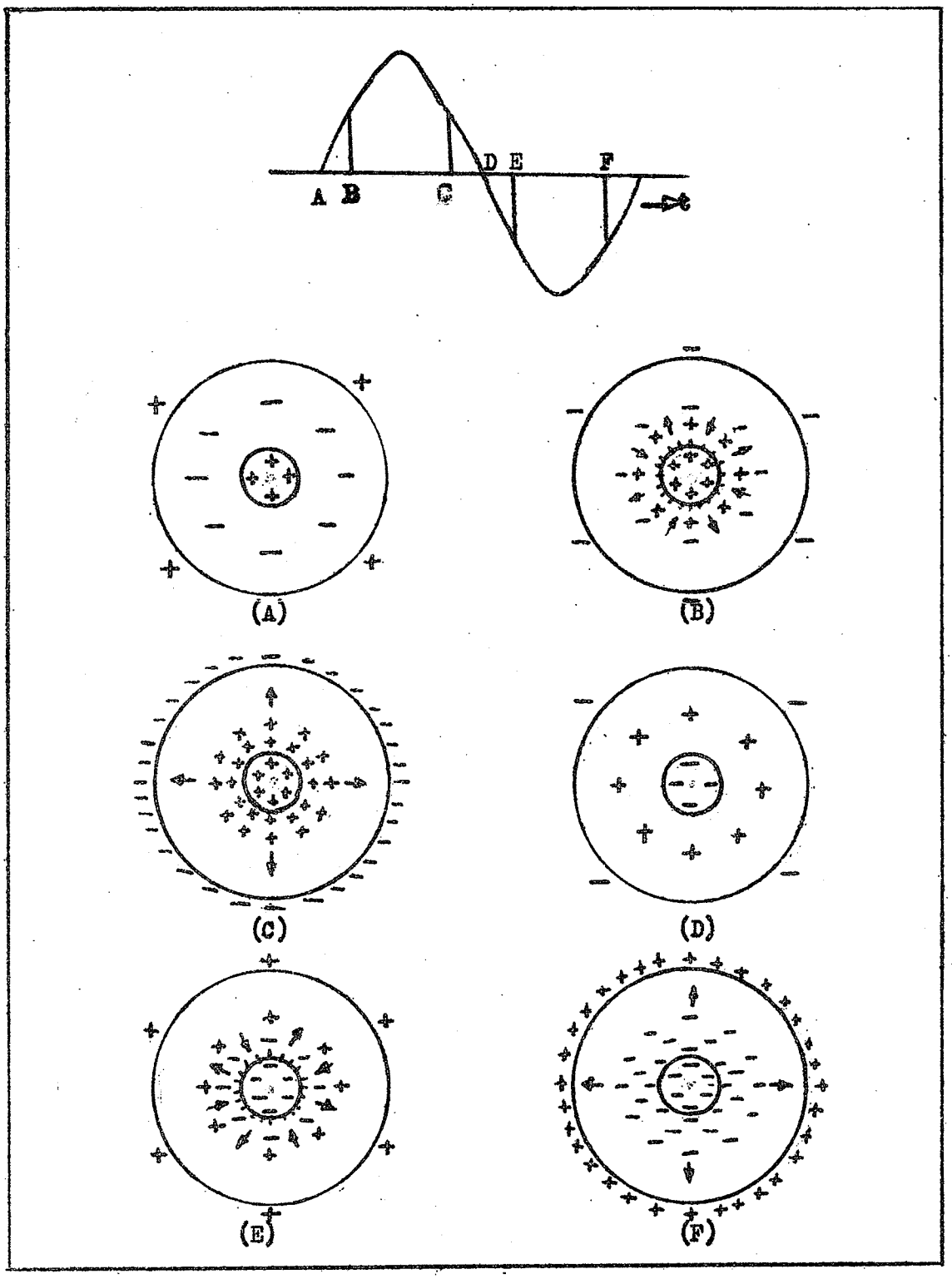

FIGURE 2.1 – A.C. CORONA SPACE CHARGE; ⟶ INDICATES MOTION OF SPACE CHARGE (CO-AXIAL CYLINDER ARRANGEMENT)

cause breakdown at the instant of zero applied voltage). As positive corona starts, the positive ions are driven outward and they neutralize the negative ion space charge. The positive ion space charge is most dense near the conductor surface during the latter part of positive corona (C). At the instant (D), lines of force begin from the positive ion space charge and end on negative bound surface charges on the conductor and cylinder. At some time (E), the field due to the combined action of space and surface charges reaches a value sufficiently high for ionization to occur at the conductor. Negative corona then begins, and the residual positive ion space charge is neutralized. The point (F), at the negative half cycle corresponds to (C) at the positive half.

During the period (B)-(C) the ionizing electrons proceed toward the conductor from the surrounding region. These electrons cause cumulative ionization and form avalanches. As a result positive ion space charge is produced which increases almost exponentially as the conductor is approached. In the negative corona period (E)-(F) the ionizing electrons are emitted from the conductor surface by positive ion bombardment and field emission. These electrons are accelerated outward producing ionization by collision. In this period

(E)-(F), the resulting positive ion space charge increases nearly exponentially with distance from the conductor. This continues until a point is reached at which effective cumulative ionization ceases. During the corona periods the motion of the charges under the influence of the applied voltage produces a component of current that superimposes on the normal capacitance charging current.

There should be a dissimilarity in the wave form of successive half cycles of current. Such dissimilarity as it occurs is due partly to the difference in the ion mobilities (positive and negative). This effect would be expected to be less pronounced for parallel wires than for co-axial cylinders.

CHAPTER III

SCHERING BRIDGE MEASUREMENTS AND RESULTS

3.1 THE CYLINDRICAL TEST CELL

The cylinder proper (Fig. 3.1) consists of a 14-foot length of 10.42 inch internal diameter extruded aluminum pipe. The guards at the ends consist of 2-foot sections of the same pipe, each having a spun aluminum end bell of the same internal throat diameter attached to it. The cylinder proper and guards are supported in a plywood frame (not shown) on which are mounted "expanded metal" screens to shield the apparatus from stray laboratory fields. A blower is mounted at one end, for the purpose of clearing ionization products from the cylinder if desired.

3.2 SCHERING BRIDGE

The circuit diagram and shielding arrangements of the Schering Bridge are shown in Fig.3.2. If the specimen is represented by a capacitance C_X and a series resistance ρ, then under balanced conditions

$$\rho = R_3 \frac{C_4}{C_S} \qquad \text{.....(3.1)}$$

$$C_X = C_S \frac{R_4}{R_3} \quad \text{..... (3.2)}$$

and the dissipation factor is

$$\tan\delta = \omega C_4 R_4 \quad \text{..... (3.3)}$$

Now,

$C_S = 103.55 \times 10^{-12}$ farads

and

$R_4 = 2652.6$ ohms

so, at 60 c/s the value of C_4 in microfarads gives directly the dissipation factor.

3.3 DESCRIPTION OF EXPERIMENTS

The test conductor sample was strung and centered in the test cell and energized from the first stage unit of the laboratory high voltage supply. As the voltage was raised in steps, the power factors (C_4 in microfarads) and values of R_3 were recorded from the bridge balance. The corresponding peak voltages were taken by direct reading of the vacuum tube voltmeter, utilizing the Standard Capacitor of the bridge circuit as a part of a capacitor divider.

Below the critical disruptive voltage the applied voltage was raised in very small steps and the bridge was balanced at each step. This was continued until the

first kick in the pointer was observed. The bridge could not be balanced properly up to some voltage after the first kick. Above this voltage the power factor increased very rapidly. Readings were continued until the Critical Visual Corona Onset Voltage was observed. For some samples readings were also taken above this voltage.

3.4 SAMPLES TESTED

Group A: Six samples of P.V.C. covered wires.

Samples	Cond. Radius (cm)	Ins. Thickness (cm)	Overall Rad. (cm)
1	0.0815	0.0380	0.1195
2	0.0815	0.0584	0.1399
3	0.0815	0.0786	0.1601
4	0.0815	0.1182	0.1997
5	0.0815	0.1320	0.2135
6	0.0815	0.1650	0.2465

Group B: Five samples of bare conductors.

Samples	No. A.W.G.	Cond. Rad. (cm)	Increase in Rad. from 0.0815 (cm)
1	14	0.0815	0.0000
2	12	0.1025	0.0210
3	10	0.1294	0.0479

Samples	No. A.W.G.	Cond. Rad. (cm)	Increase in Rad. from 0.0815 (cm)
4	8	0.1632	0.0817
5	6	0.2057	0.1242

Group C: Three samples of #22 A.W.G. wires.

Samples	Type	Cond. Dia. (mil)	Overall Dia. (mil)
1	Bare	25.35	25.35
2	P.V.C. Covered	25.35	43.35
3	Polyethylene Covered	25.35	43.35

3.5 TEST RESULTS

1. Power Factor Characteristics:

The Power Factor Characteristics of the p.v.c. covered conductors (Group A) are shown on page 25 and those of the bare conductors (Group B) are shown on page 26. The data are given in tabular form in appendix A4.1(1) and A4.1(2) respectively.

The two sets of curves show a fundamental difference. In the first set for each conductor the power factor remains more or less constant up to a certain critical voltage and then rises very quickly. This is due to the low loss properties of the insulation. After the critical voltage the rise is mainly because of the

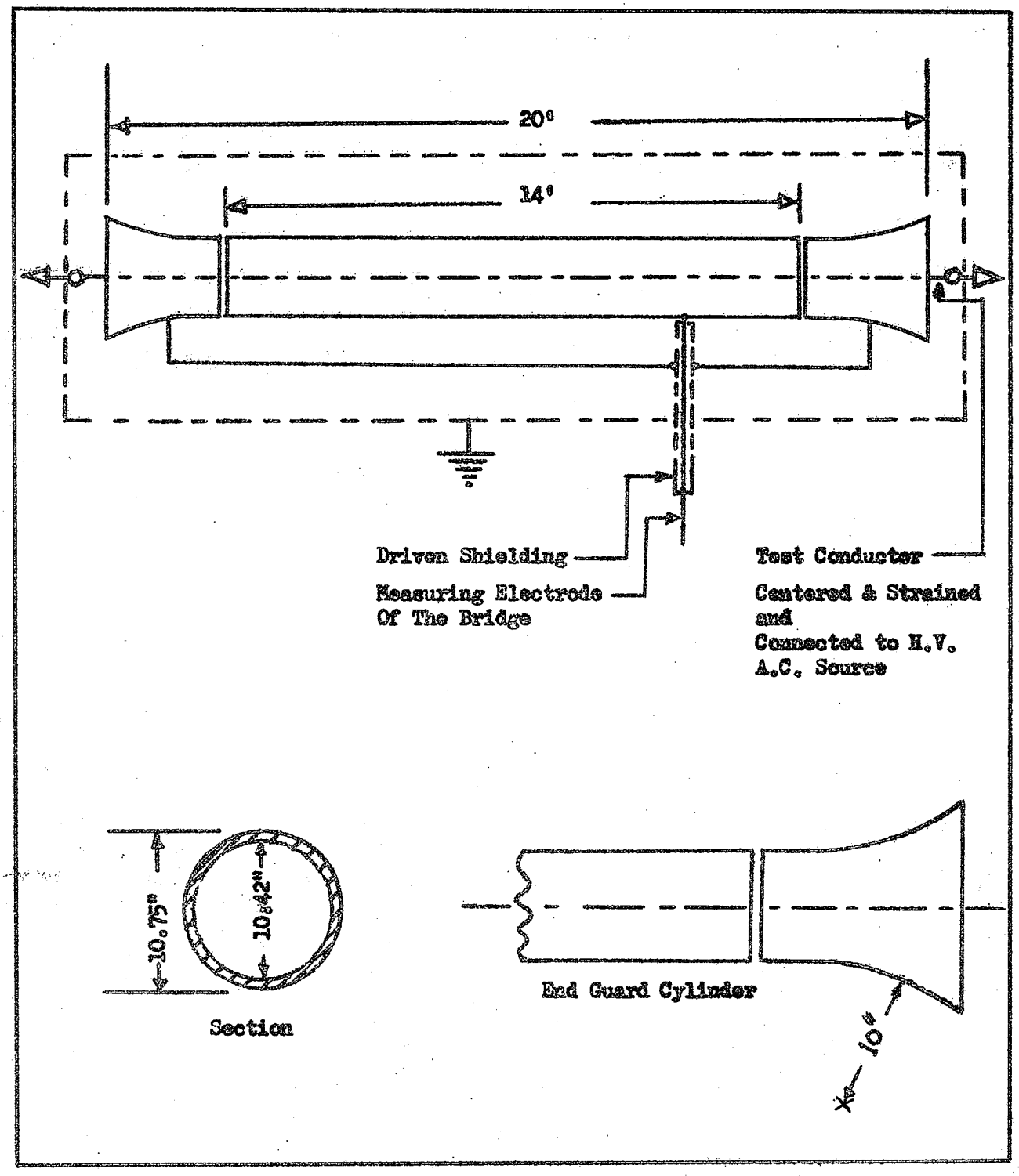

FIGURE 3.1 - THE TEST CELL

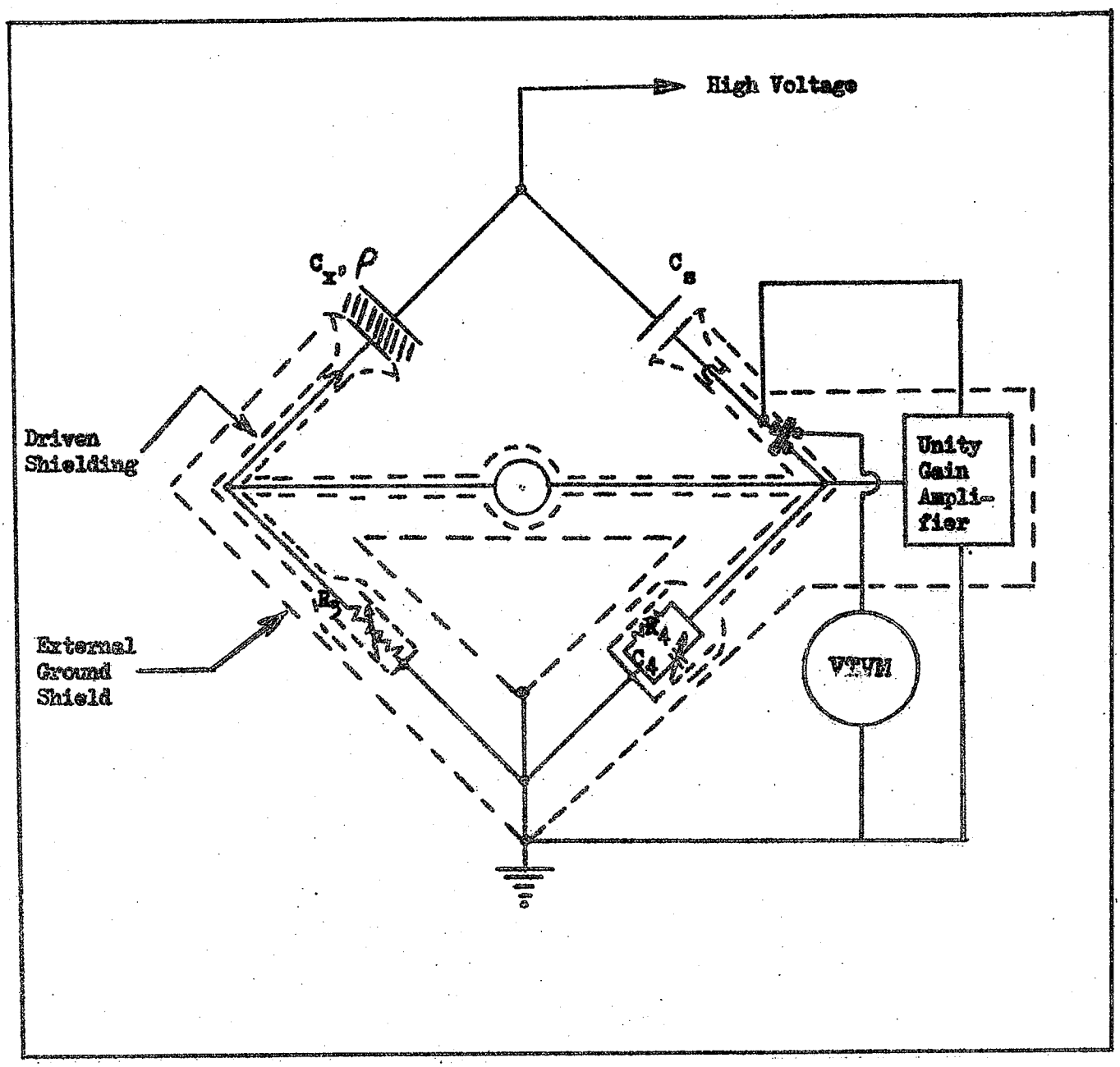

FIGURE 3.2 - SCHERING BRIDGE

ionization of the air near the conductor surface. The set shows gradual increase in ionization with voltage. When cumulative ionization starts the power factor rises sharply.

The Power Factor Characteristics of the #22 A. W.G. wires are shown on page 27. Both the insulated conductors have shown better characteristics than the bare ones. Between the insulated conductors the Polyethylene covered one has shown better results. (Explanation of this is given in Chapter V).

2. Power Loss Characteristics:

(a) Bare Conductors - With the bare conductor inside the co-axial cylinder the equivalent circuit

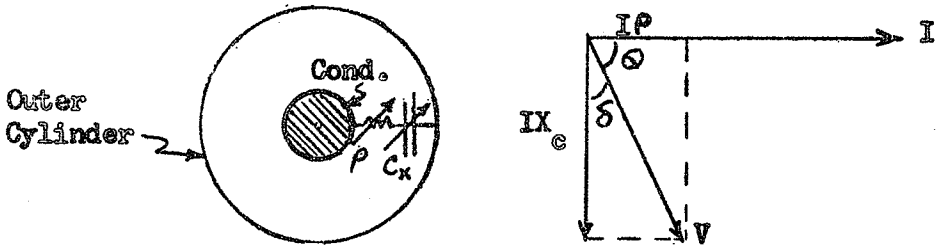

Figure 3.3:- Equivalent Circuit and Vector Diagram (Bare Conductor inside Co-axial Cylinder).

and the associated vector diagram are shown in figure 3.3. The quantities ρ and C_X would change with voltage, but they are measurable. From the vector diagram,

Power Loss = VI CosΘ

$I \fallingdotseq V\omega C_X$ & $\text{Cos}\Theta = \text{Sin}\delta \fallingdotseq \tan\delta$

$$P = V^2\omega C_X \tan\delta = \frac{(KVP)^2}{2}\omega C_X \tan\delta \text{ watts...(3.4)}$$

C_X is in microfarads.

(b) With the insulated conductor inside the concentric cylinder, the equivalent circuits are shown in figure 3.4. As for the bare conductors, the power loss,

$$P = \frac{(KVP)^2}{2}\omega C_{X_i} \tan\delta \text{ watts.....(3.4)}$$

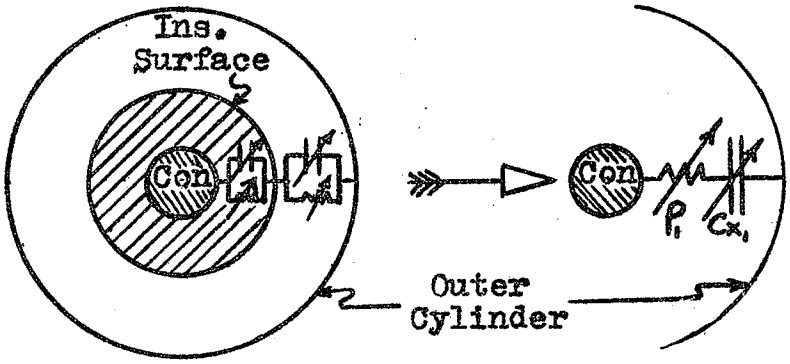

Figure 3.4:- Equivalent Circuits (Insulated Conductor Inside Co-axial Cylinder).

In equation (3.4) all the quantities in the R.H. side are known. For samples 3 and 4 of Group A and 1 and 4 of Group B, the power losses are calculated from

this equation. The results are shown in appendix A4.1(4). The calculations are valid up to the point where we can write $\cos\phi = \sin\delta \fallingdotseq \tan\delta$ i.e. nearly up to visual corona voltage. The power losses are also plotted against KVP as shown on page 28. From the graphs it is found that for #14 wire significant loss starts at about 19 KVP; but if this wire is insulated with p.v.c. of thickness 0.0786 cm., the loss starts at about 35 KVP. The power loss characteristic of this insulated conductor is even better than that of #8 bare wire having a greater overall diameter.

3. Visual Corona Onset Voltage and Gradient Characteristics:

The onset voltages for bare and insulated conductors are calculated from*

$$V_C = E_C r_i \ln (R/r_i) \text{ KVP} \quad \ldots\ldots\ldots\ldots\ldots\ldots (2.4)$$

and

$$V_C = E_C r_i \left[\frac{\ln r_i/r}{K} + \ln R/r_i\right] \text{ KVP} \quad \ldots\ldots (3.5)$$

respectively, where,

r_i = Total Radius

r = Cond. Radius

K = Rel. Permittivity of P.V.C.

= 5.7

---

* This is an extension of equation No.A3.1 shown in appendix 3 and justification of use is given in Chapter IV.

and

$$E_C = 31m\delta\left(1 + \frac{0.308}{\sqrt{\delta r}}\right) \text{ KVP/cm} \quad \ldots\ldots\ldots\ldots (2.3)$$

(with m = 1)

The calculated and measured results are compared in graph 3.5 on page 29. The ratio of V_C (measured) to V_C (calculated) is defined as m. It is interesting to note that for the bare conductors m varied from 0.93 to 0.958 with an average of approximately 0.95 and for the insulated conductors it varied from 0.94 to 0.957 with the same average.

The calculations show that for both types of wires the critical gradients follow equation (2.3), which is plotted on page 30 (with m = 1, δ = 1) as a function of overall radius.

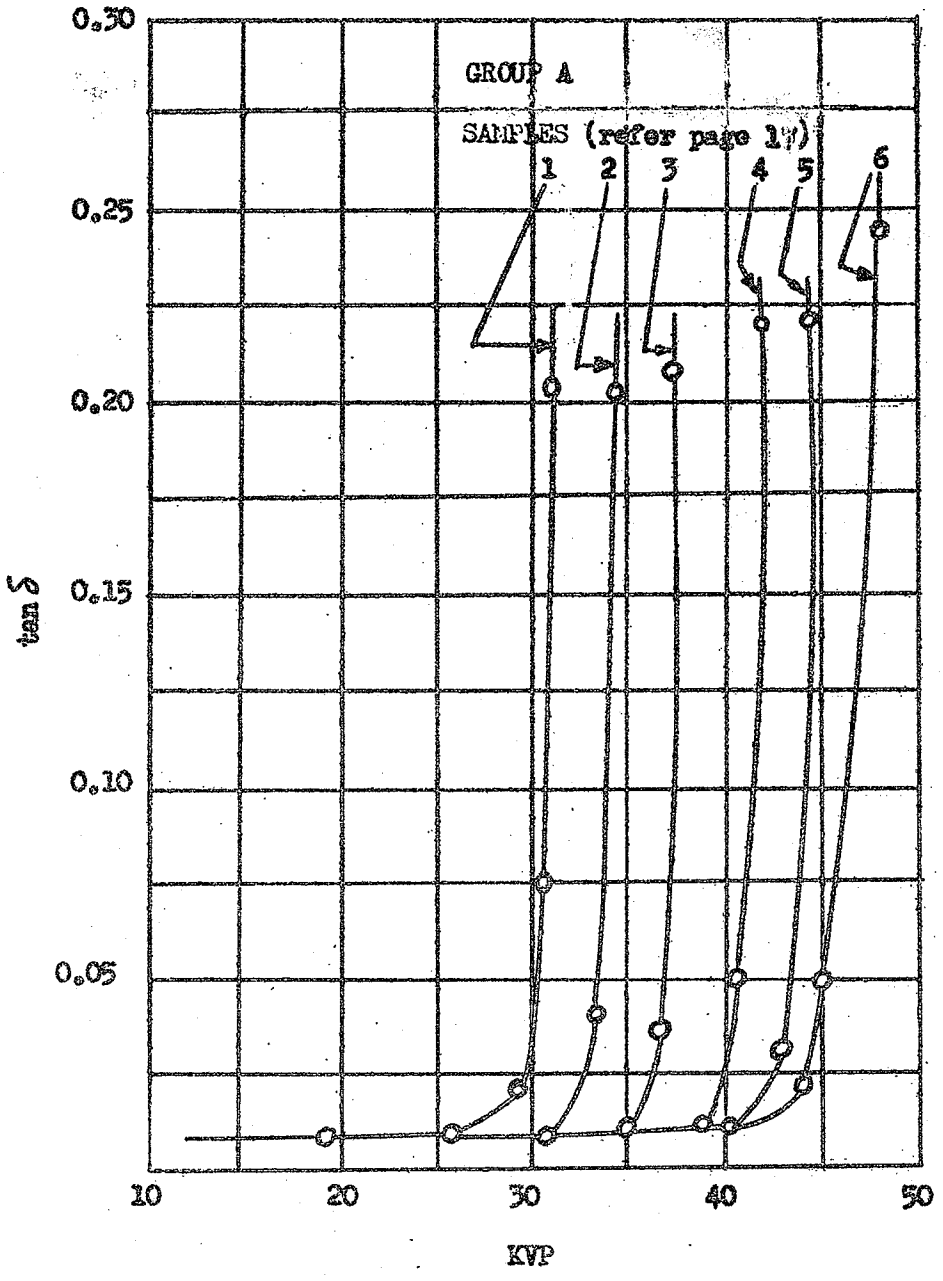

GRAPH 3.1 - POWER FACTOR CHARACTERISTIC OF P.V.C. INSULATED CONDUCTORS

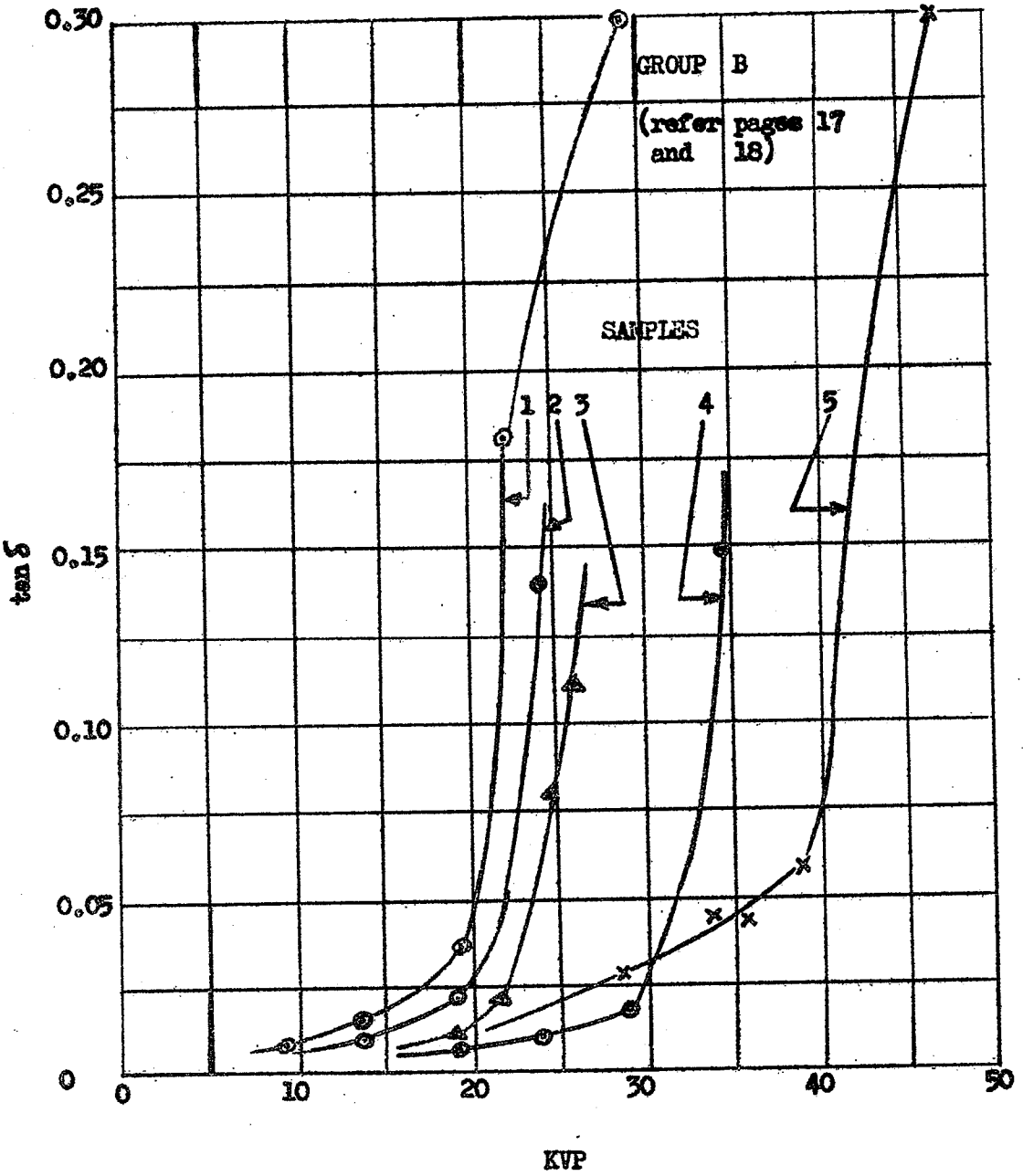

GRAPH 3.2 - POWER FACTOR CHARACTERISTICS OF BARE CONDUCTORS

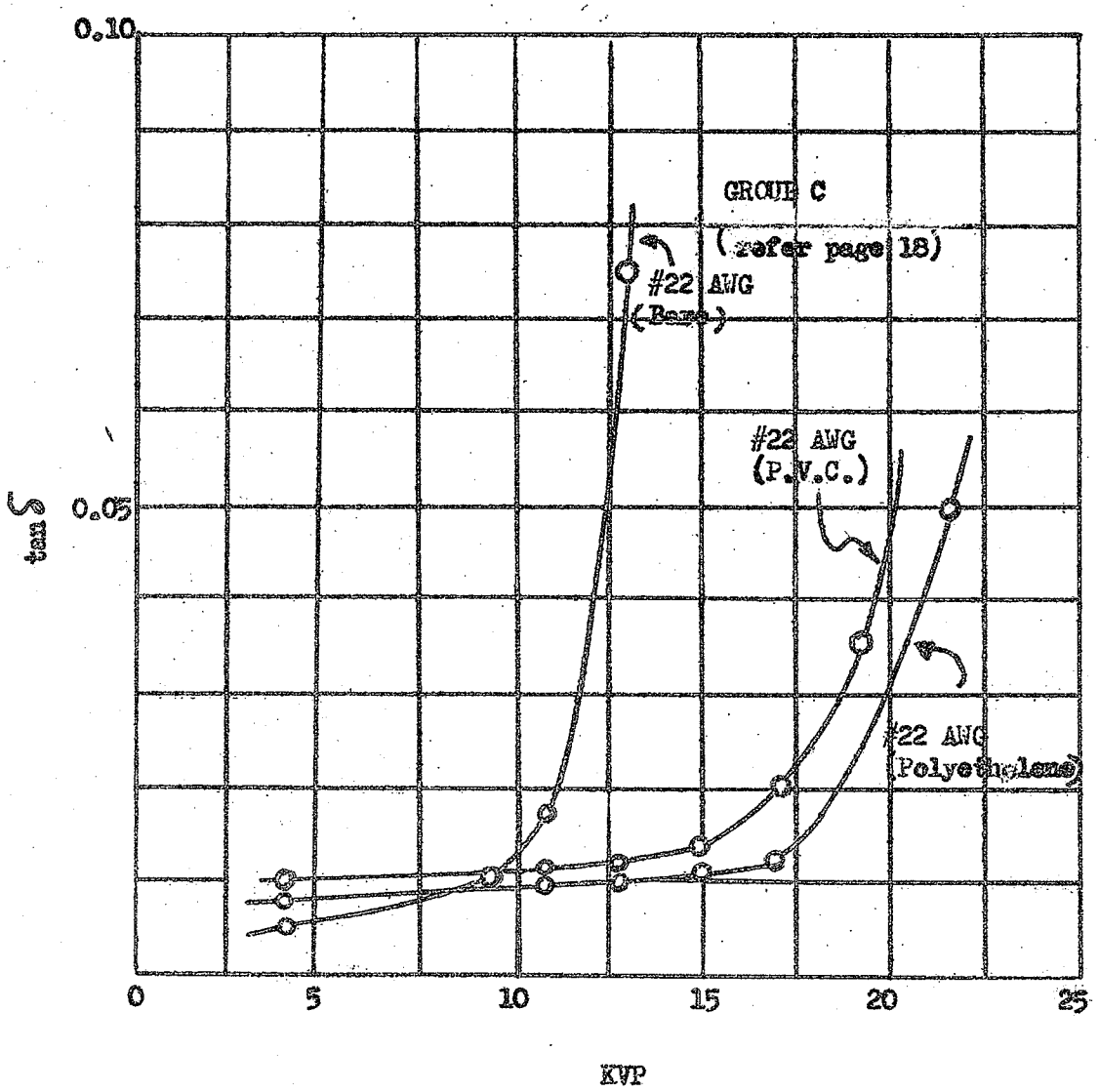

GRAPH 3.3 - POWER FACTOR CHARACTERISTICS
OF # 22 A.W.G. WIRES

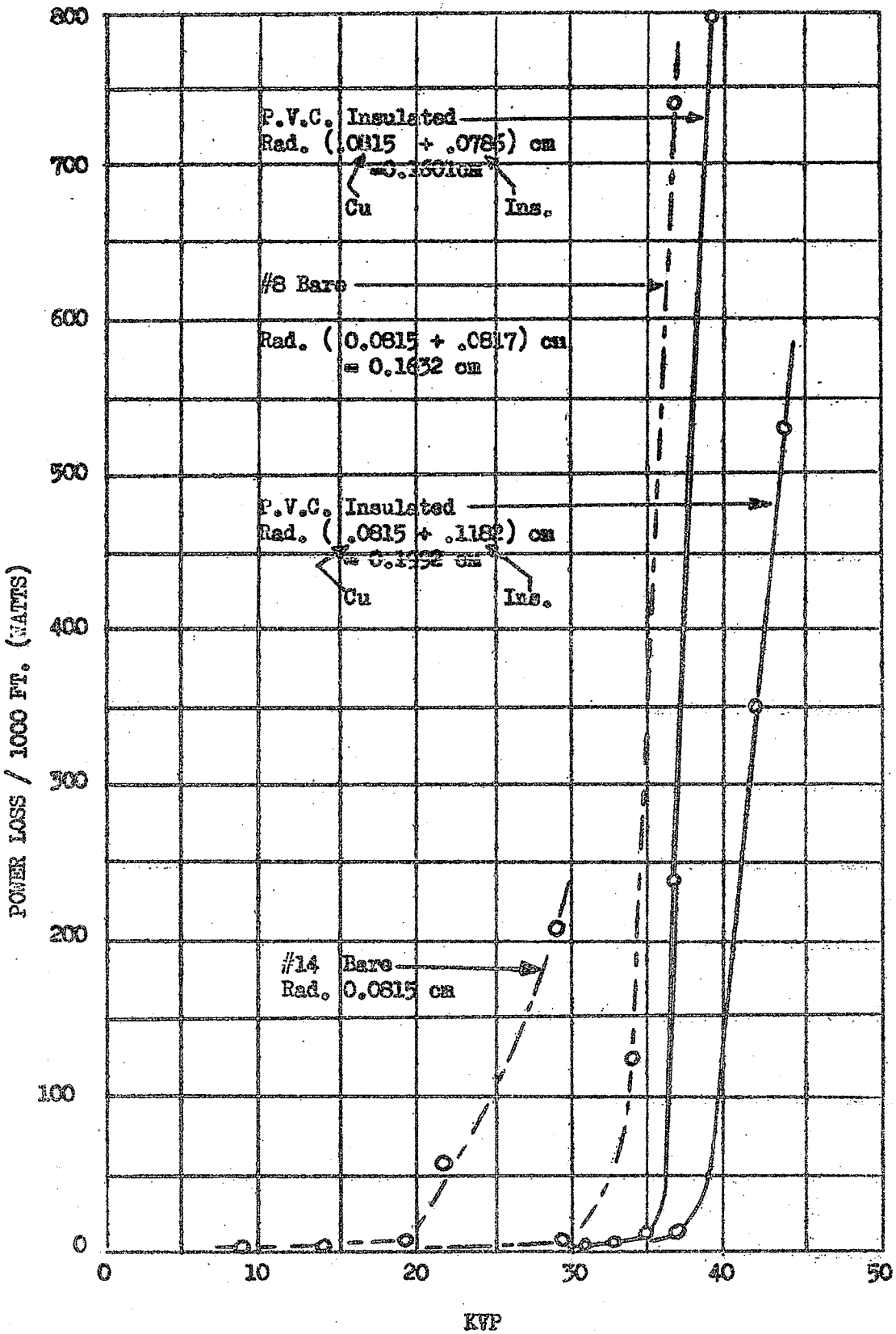

GRAPH 3.4 - POWER LOSS CHARACTERISTIC

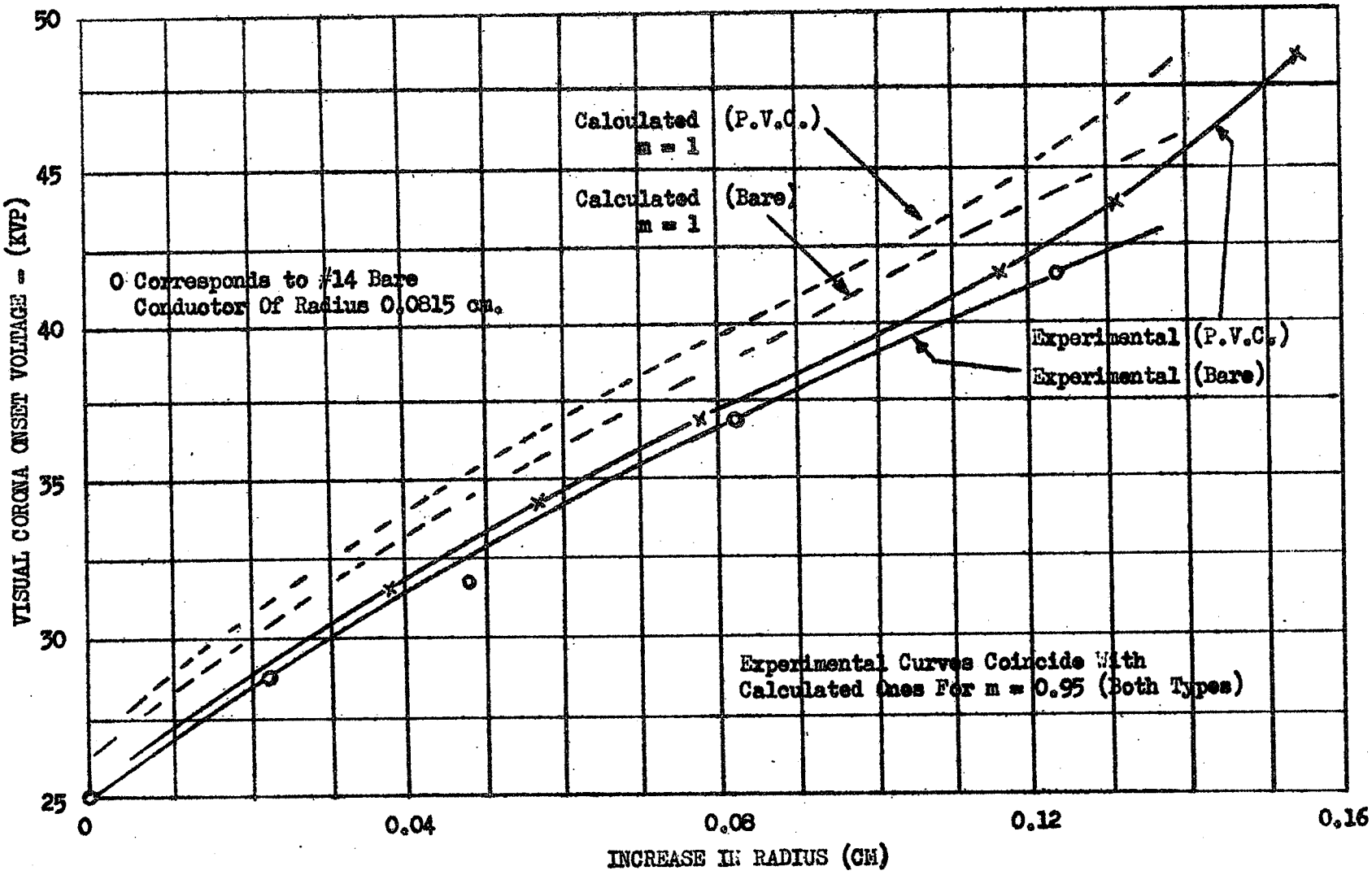

GRAPH 3.5 - VISUAL CORONA VOLTAGE CHARACTERISTICS

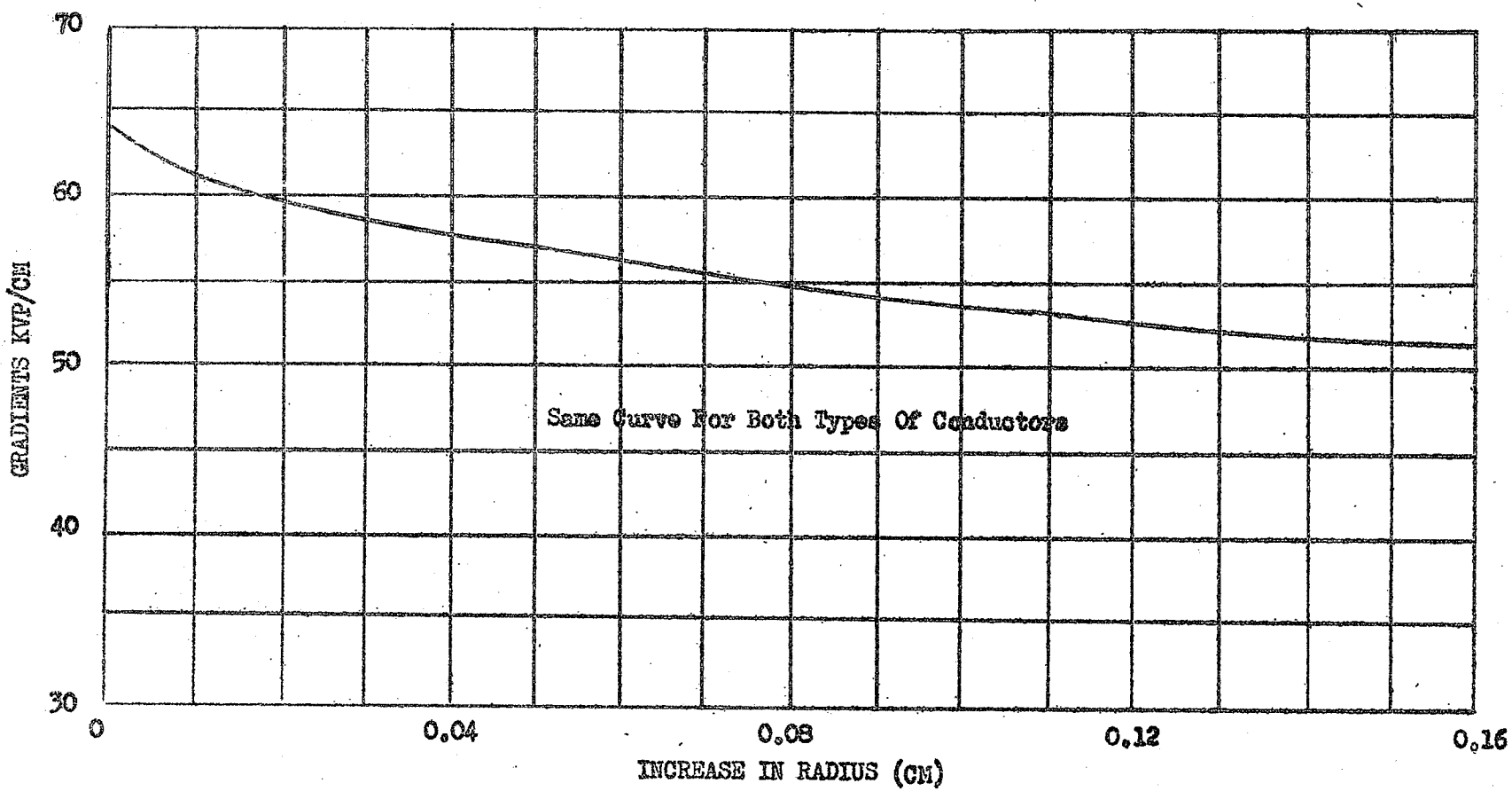

GRAPH 3.6 - VISUAL CORONA GRADIENT CHARACTERISTICS

CHAPTER IV

RADIO INFLUENCE VOLTAGE MEASUREMENTS

4.1 RADIO NOISE METER

"Radio noise" is radio frequency energy radiated from electrical equipment usually at frequencies covering the commercial broadcast band. It becomes audible noise when detected at a radio receiver. The degree to which this noise is objectionable depends on the bandwidth of the receiver and the response characteristics of the human ear.

In a Radio Noise Meter an attempt is made to measure "nuisance value" taking the above factors into account and giving a quantitative result. The Radio Noise Meter is, therefore, a superheterodyne receiver (without automatic volume control) with a meter which measures the peak, quasi-peak, rms, or average value of the intermediate-frequency stage output. The quasi-peak output is determined by the charge and discharge constants of the detector circuit, which are selected to correspond to nuisance value.

In the measurements here, a Ferris meter (Radio Noise and Field Strength Meter, Model 32-D,

Serial No. 86) was used, using the "quasi-peak" setting. In using the meter frequent calibration with a standard source is necessary for consistent results.

4.2 EQUIPMENT

Radio interference from corona on insulated and bare conductors was studied under the same concentric cylinder arrangement as was used for power factor measurements. The circuit is represented in figure 4.1. The figure shows that high voltage was applied between the conductor and cylinder, the conductor being at the high potential. In this method corona current rather than 'RIV' is measured. Reversing the cylinder and conductor with respect to applied voltage might make the pulse measurement problem easier. However, that was not feasible and the method used was sufficient for comparison purposes.

The 'RN' meter was used as a r-f tuned voltmeter at 1 mc. (dummy antenna measurements) and in all the steps the manufacturer's advice was followed. The high-pass filter circuit was used to eliminate the 60-cycle component of the current wave. The double-channel

oscilloscope showed the 1 mc. pulse components and the voltage wave shapes. In accordance with the Canadian and U.S. standards, the 1-ms charge time constant was used in all the measurements.

4.3 SAMPLES TESTED

Group A - Samples 1 to 5

Group B - Samples 1 to 3 and a #8 A.W.G. bare conductor having diameter - 130 mils.

4.4 TEST RESULTS

1. Radio Influence Voltage Characteristics:

The measured values of 'RIV' for different conductors are given in tables in appendix A4.2. It is usual to plot 'RIV' logarithmically against voltage, and this has been done in graph 4.1 on page 37. There is a difference in the nature of the curves for the two sets of conductors. Immediately after inception, the curves for the insulated conductors rise very sharply; then a few peaks occur. The rise of the curves for the bare conductors is quite gradual.

For the bare conductors within the experimental range, the 1 mc. interference occurred first at the negative peaks of the voltage and then also at the positive peaks at higher voltages. For the insulated conductors

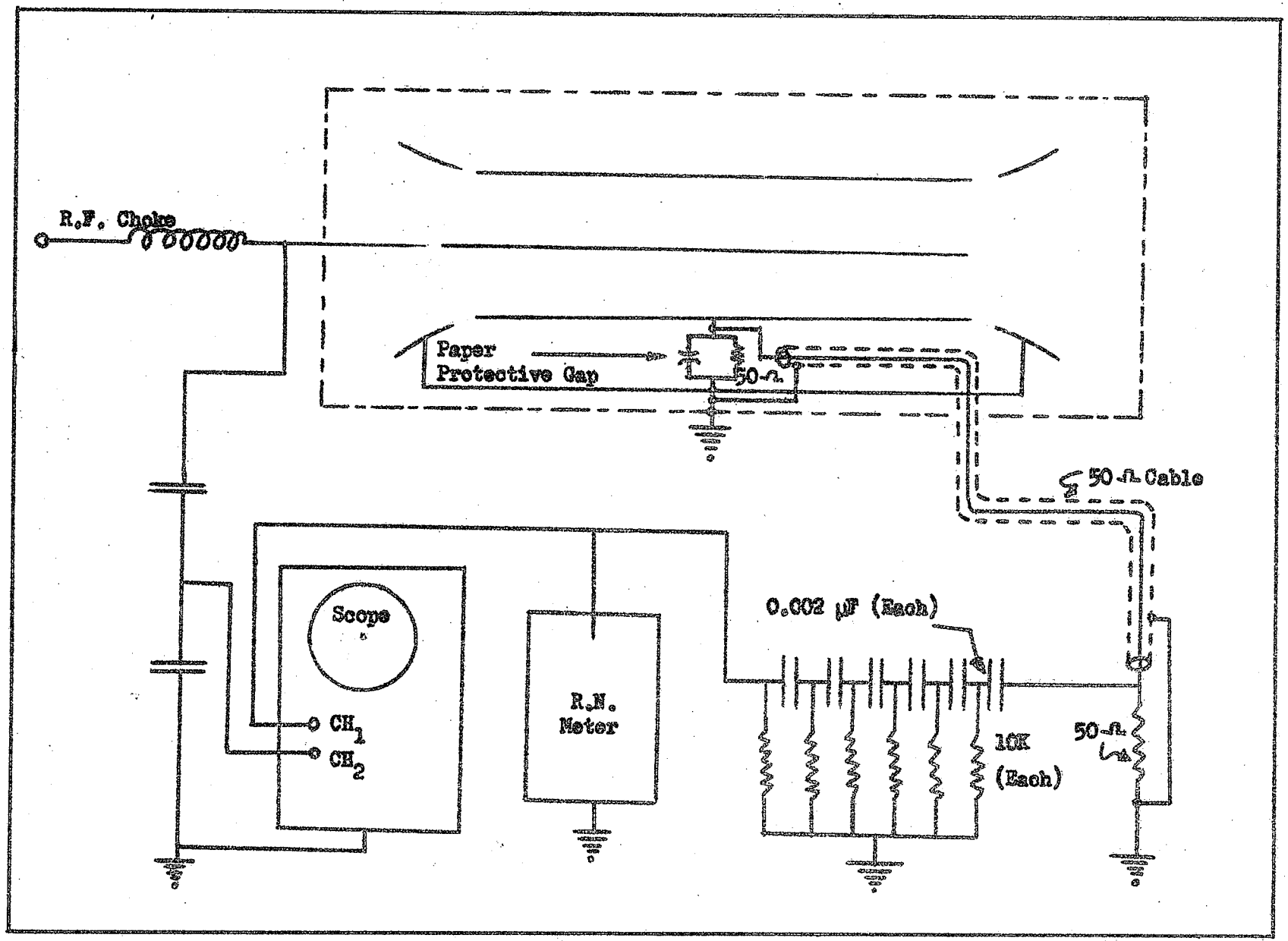

FIGURE 4.1 – CIRCUIT DIAGRAM FOR RADIO NOISE TESTS

the reverse process was observed.

2. Radio Noise Inception Voltage and Gradient Characteristics:

The 1 mc. radio noise inception voltage and gradient characteristics for both types of conductors are shown as a function of increase in radius (from that of #14 A.W.G. bare wire) on page 38 and 39 respectively. For the insulated conductors higher values of voltages and gradients were necessary to cause noise inception. Moreover, in each case the gradients were found to be a function of overall radius. For both types of conductors they were slightly less than those given by Peek's formula for visual corona (Eq.2.3).

3. Radio Influence Gradient Characteristics:

Corona is directly related to the stress and therefore, the data for samples 1 and 2 of Group A and 1 and 3 of Group B are represented on page 40, as plots of influence voltage against stress at the wire surface. The curves for the insulated conductors show regular peaks. The curves for the bare conductors may be approximated as straight lines showing that they follow a law of the form,

$$RIV = R\,(E-G) \qquad \text{.....(4.1)}$$

where R is a function of radius, E is the onset stress in KVP/cm., (which is another function of radius), and G is the applied stress in KVP/cm. This shows that the rate of increase of influence voltage with stress increases with the wire radius.

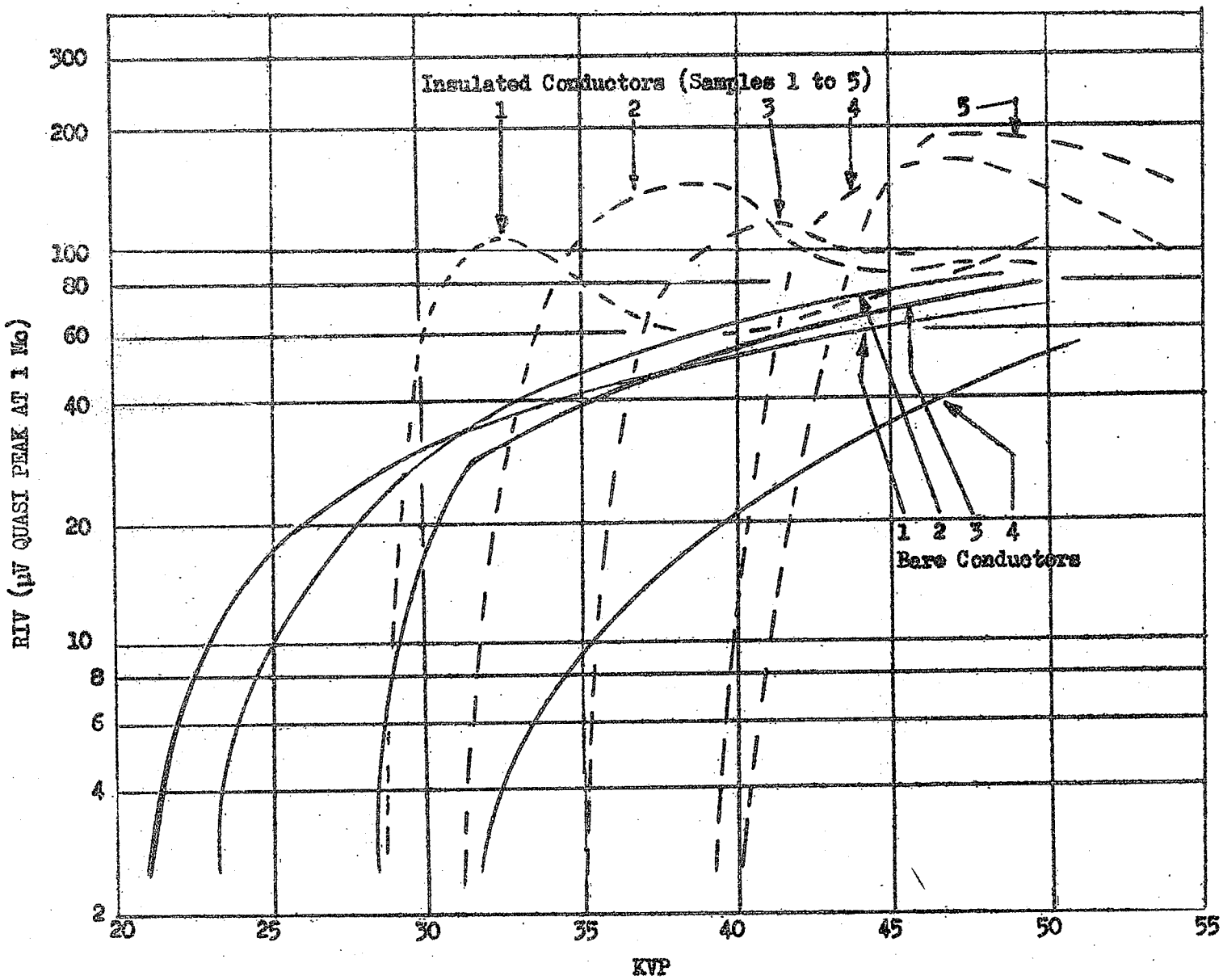

GRAPH 4.1 - RADIO INFLUENCE VOLTAGE CHARACTERISTICS

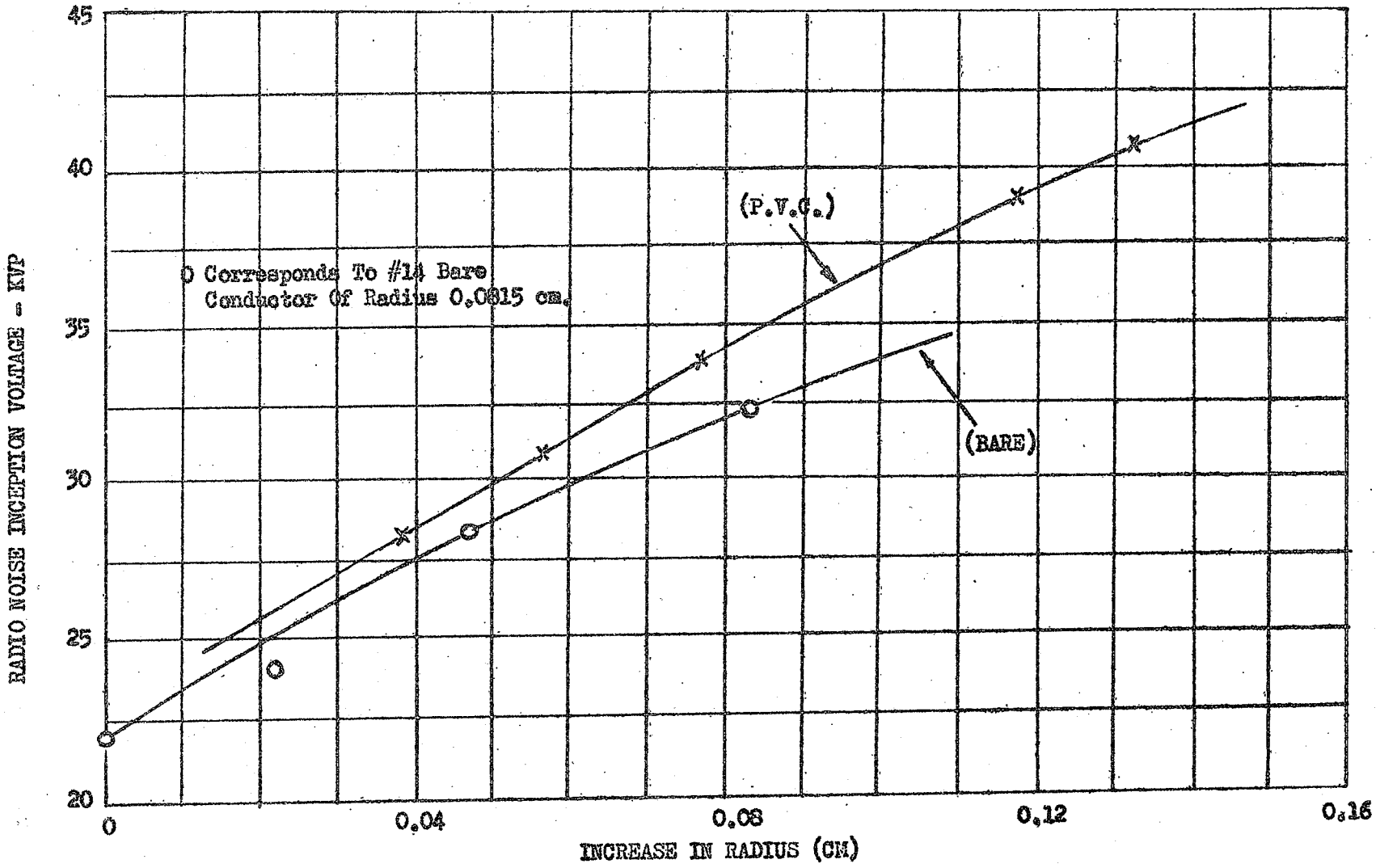

GRAPH 4.2 - RADIO NOISE INCEPTION VOLTAGE CHARACTERISTICS

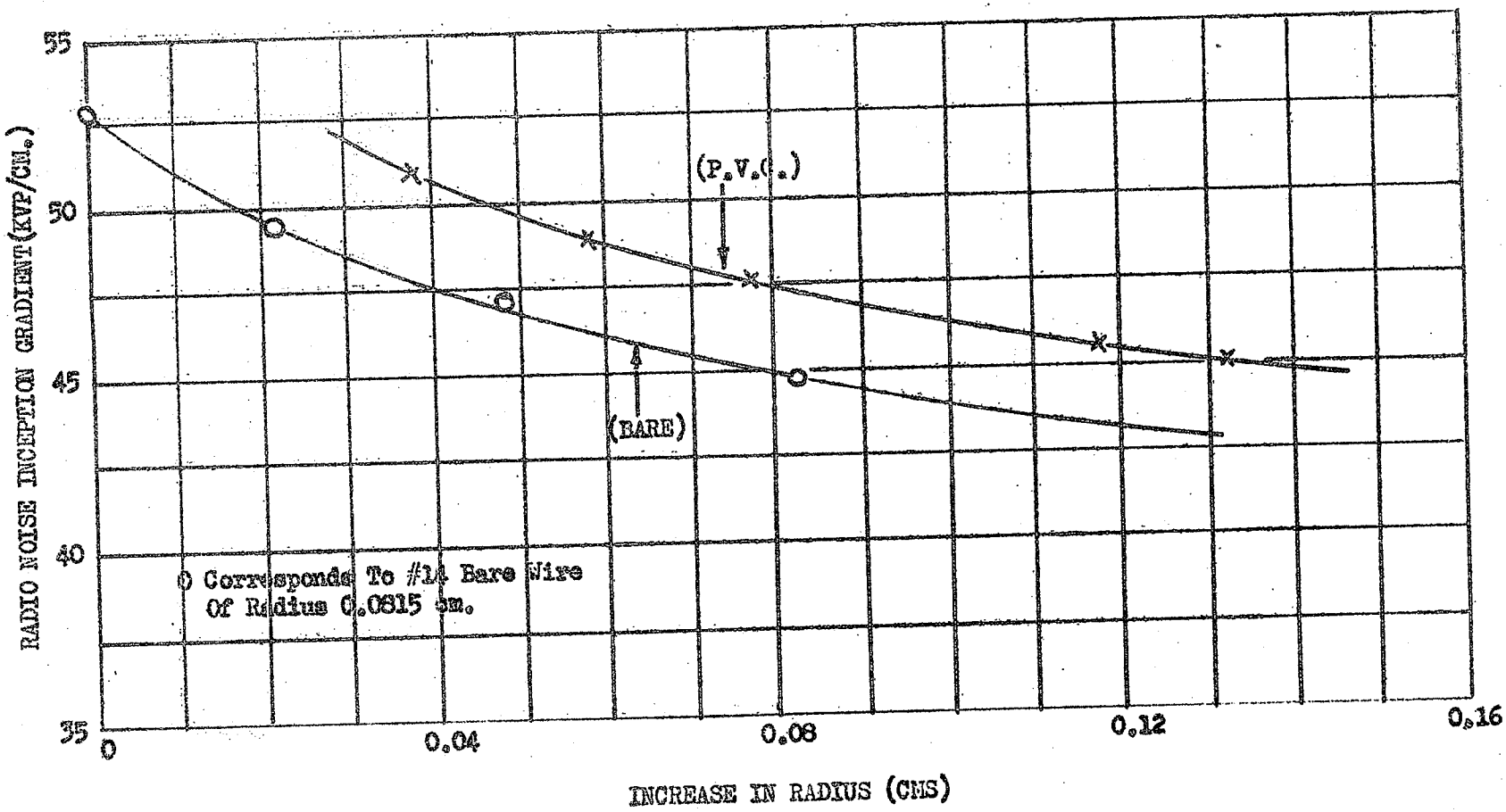

GRAPH 4.3 - RADIO NOISE INCEPTION GRADIENT CHARACTERISTICS

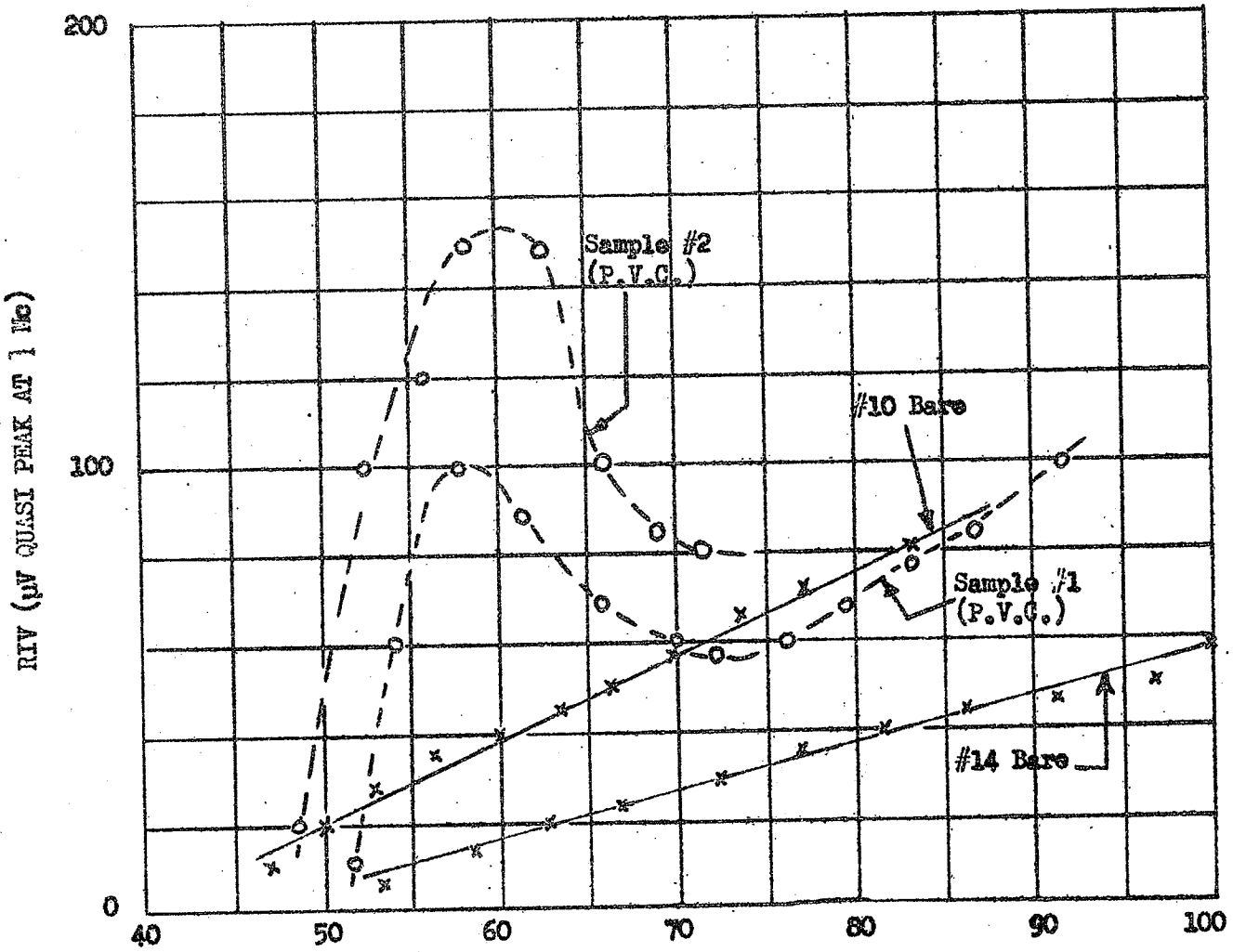

GRAPH 4.4 - RADIO NOISE GRADIENT CHARACTERISTICS

CHAPTER V

EXPLANATION OF OBSERVED FACTS AND DISCUSSION

5.1 PROPERTIES OF DIELECTRICS

Before proceeding to give any explanation of the observed facts, it is necessary first to discuss some of the properties of dielectrics and their behaviour under a.c. field at power frequency. In the concentric cylinder arrangement let the dielectric be air. At an instant when the wire is at a positive potential with respect to the outer cylinder, radial flux lines originating from the positive charges on the conductor will terminate on an equal number of negative charges on the cylinder. Since there is no flux line parallel to the axis, there would be no force parallel to it. The electric field (normal to the surface) at any point in between

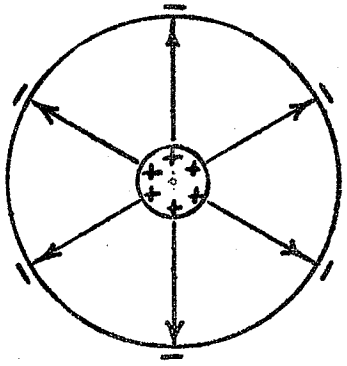

Figure 5.1:- Flux Line Terminating on Opposite Charges (Co-axial Cylinders)

the cylinders may be given by

$$E = \frac{D}{\epsilon_o} \quad \text{.....(5.1)}$$

where, D is the flux density and ϵ_o is the absolute permittivity of air ($\approx$ vacuum). D is at a maximum at the conductor surface and E would, therefore, be maximum there (ϵ_o being a constant).

Now let us replace the air by an insulating material. Because of its physical structure this insulating material will contain some electric dipoles of some kind. The electric field produced by the applied voltage exerts forces on these dipoles causing them to rotate and align themselves with the electric field.

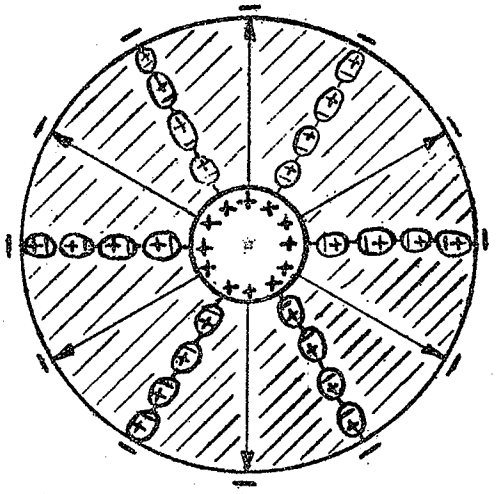

Figure 5.2:- Dipole Orientations.

New lines of flux are set up between the aligned dipoles and terminate on additional charges on the conductor and the cylinder. The electric flux density can now be written as:-

Total flux density	=	Flux density in air (≈ vacuum)	+	Flux density from dipole orientations

$$D = \epsilon_0 E + P \qquad \text{.....(5.2)}$$

The quantity P is known as the Dielectric Polarization. It is the flux density added by the aligned dipoles.

In the preceding paragraphs the dipoles were considered to be rotating when the electric field was applied. However, in real dielectrics all of the dipoles may be induced and present only when the electric field is applied. Accordingly, polarization is of several types, but it is always convenient to consider the insulation as being full of dipoles randomly oriented (due to thermal agitation) under normal conditions. Dipole orientation occurs under the action of an applied field and this continues until they are aligned with the electric field.

It is now defined that

$$D = \epsilon E \qquad \text{.....(5.3)}$$

where ϵ is the absolute permittivity of the material. Therefore,

$$\epsilon E = \epsilon_o E + P \quad \text{.....(5.4)}$$

Dividing through by the electric field intensity E,

$$\epsilon = \epsilon_o + P/E \text{ Farads/meter} \quad \text{.....(5.5)}$$

The polarization and the electric field intensity are usually parallel, hence the absolute permittivity of the material is always greater than that of free space. Also, a material containing a high density of dipoles (especially the polar substances) will have a high degree of polarization and consequently a large dielectric constant.

Dividing equation (5.5) through by ϵ_o,

$$K = \frac{\epsilon}{\epsilon_o} = 1 + P/D \quad \text{.....(5.6)}$$

K is a dimensionless constant and is defined as the relative dielectric constant or relative permittivity of the material. From equation (5.6) it is evident that K is always greater than unity.

In the previous treatment the insulation was considered to behave as a perfect dielectric having no loss. However, there is no such material as a perfect dielectric. In fact, when subjected to alternating voltage, in addition to the normal charging current there is a conduction

current, so that one may replace the dielectric by a perfect capacitor shunted by a resistor.

In most materials, however, the dielectric behaviour differs from this simple form also, indicating the presence of other sources of dielectric loss. At present a complex permittivity

$$\epsilon^* = \epsilon' - j\epsilon'' \quad \text{.....(5.6)}$$

and a corresponding complex dielectric constant

$$K^* = \frac{\epsilon^*}{\epsilon_o} = K' - jK'' \quad \text{.....(5.7)}$$

are introduced to describe the properties of the material. The term K" is the loss factor. It should be zero for a perfect dielectric with no loss. On the basis of ϵ^* and K^* so defined the total current at a voltage V can be written as:-

$$I = j\omega K^* C_0 V = (j\omega K' + \omega K'') C_0 V \quad \text{.....(5.8)}$$

where C_0 is the capacitance with a vacuum dielectric. The loss tangent is:-

$$\tan\delta = K''/K'$$

The loss tangent will depend on the following well recognized properties, or conditions of insulation, if present:

1. Normal conductivity
2. Dielectric absorption

3. Absorbed moisture

4. Gaseous ionization.

However, in the experiments tanδ was found to remain more or less constant up to the RIV inception voltage and it will be reasonable to take K as a constant at least up to this voltage.

5.2 CRITICAL GRADIENTS AND VOLTAGES

Having this theory of dielectrics in mind one may now consider a conductor of radius r with an insulation thickness $r_i - r$ in the co-axial cylinder arrangement. Under the action of the electric field (positive) the dipole alignment will be as shown in figure 5.3.

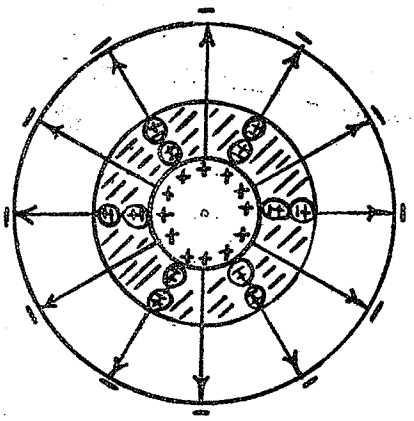

Figure 5.3:- Flux Lines From Insulation Surface to Cylinder (Co-axial Cylinders).

Applying Gauss's Law, (the surface integral of the flux density over a closed surface is equal to the

volume integral of the charge density contained within that surface i.e. the total charge contained therein), at the surface of separation of the two dielectrics it may be written that

$$\oint K \epsilon_o \overset{S*}{E}_{ins} \cdot da = Q = \oint \epsilon_o \overset{S}{E}_{air} \cdot da \ldots\ldots (5.10)$$

From which,

$$\overset{S}{E}_{air} = K\overset{S}{E}_{ins} \ldots\ldots\ldots\ldots\ldots\ldots\ldots\ldots\ldots\ldots (5.11)$$

That is, the direct effect of polarization is to increase the field just outside the insulation K times the field just inside. The field distribution in air is dictated by:

$$E_{air} = \frac{V}{x\left[\ln r_i/r/K + \ln R/r_i\right]} \text{ KVP/cm} \ldots (A3.1)^{**}$$

and that inside the insulation is given by:

$$E_{ins} = \frac{V}{x\left[\ln r_i/r + K \ln R/r_i\right]} \text{ KVP/cm} \ldots (A3.2)^{**}$$

In both the cases x is the distance from the centre of the conductor and V is the applied voltage.

If one now considers a bare conductor of radius r_i (being equal to the overall radius of the insulated conductor) the field distribution is determined by:

---

* S means surface.

** Derivations of these equations are given in appendix 3.

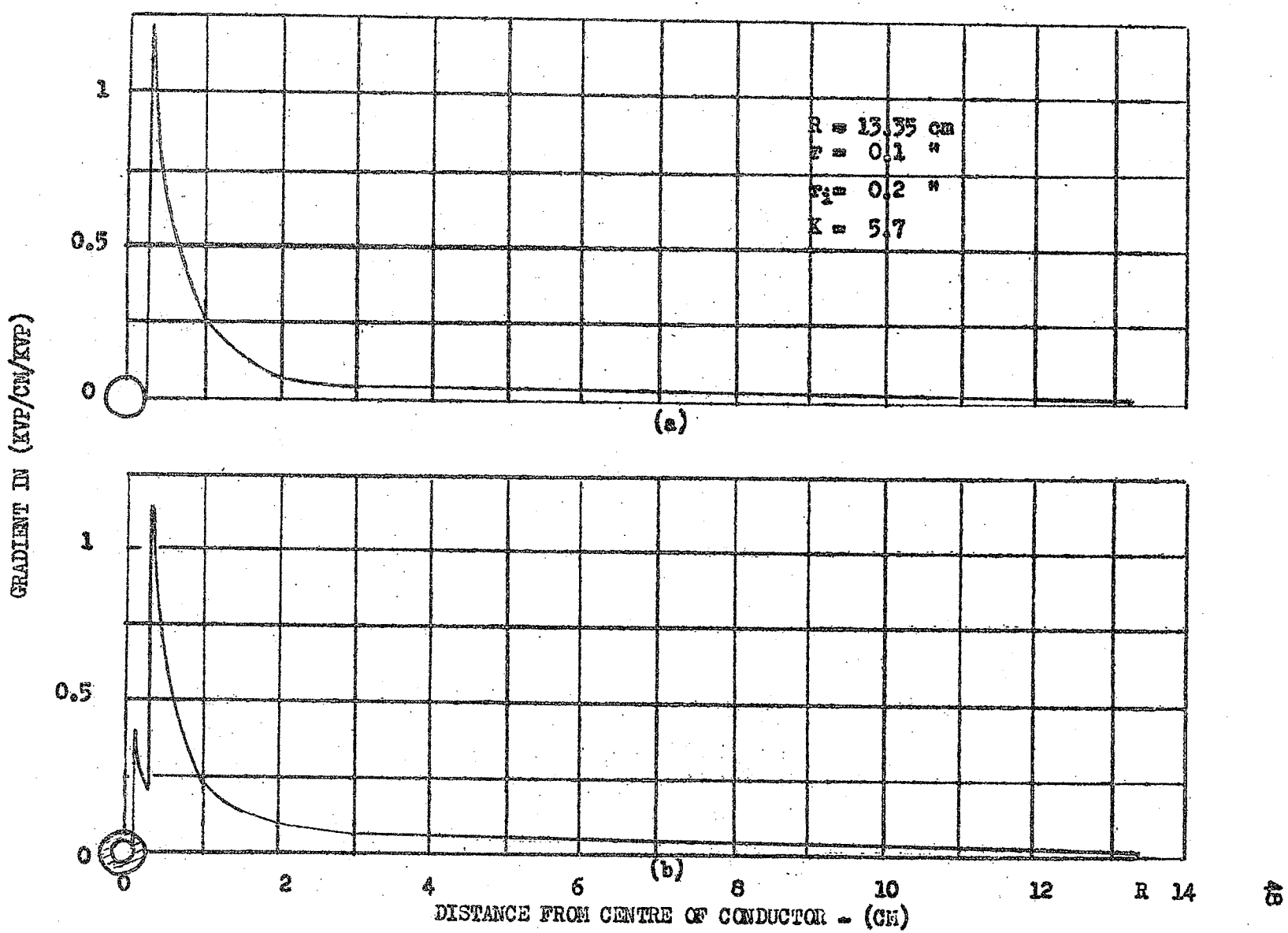

GRAPH 5.1 - FIELD DISTRIBUTION - (a) BARE CONDUCTOR
(b) INSULATED CONDUCTOR (CO-AXIAL CYLINDERS)

$$E = \frac{V}{x \, (\ln R/r_i)} \qquad \ldots\ldots\ldots\ldots\ldots\ldots\ldots\ldots (5.12)$$

Applying equations (A3.1) and (A3.2) for the insulated conductor and (5.12) for the bare conductor the field distributions are shown in graph 5.1. From these equations and also from the above mentioned curves it is evident that even if corona or RIV inception starts at the same gradient for both types of conductors having the same overall diameters, the voltage to produce that gradient for the insulated conductor would be higher than that for the bare conductor. Experiments, however, show that for the samples tested besides higher voltage, higher gradient is required for the insulated conductors to cause RIV inception (Ref: Graph 4.3). This can possibly be explained as follows:

During the negative half of the voltage wave the free electrons which are always present in the atmosphere due to ultra-violet, cosmic and other radiations will be expelled from the region of the conductor and will not be available for continued ionization in this high stress region. The necessary electrons, therefore, must come from the conductor. The positive ions which are accelerated by the electric field towards the wire will collide with gas atoms. However, because the mass of the gas ion and atom are essentially the same, the

ion loses almost half its kinetic energy in an elastic* collision. Because at every collision it gives up half the energy acquired from the electric field between collisions, the ion energy is always quite small. As a result, the positive ions seldom acquire sufficient energy to produce inelastic** collisions.

However, if the voltage is raised, the positive ions will be sufficiently accelerated in the intense field near the conductor. These accelerated positive ions will gain enough energy to cause secondary emission from the conductor surface. The electrons emitted in this process will cause ionization by collision.

Electrons may also be produced by field emission. Irregularities and projecting points are always present on a conductor surface. The highly concentrated electrostatic fields around these irregularities and projections may cause field emission.

---

* An elastic collision is that for which the total kinetic energy of the two particles is the same after collision as before collision.

** For an inelastic collision the total kinetic energy of the system is not conserved. The difference is the excitation or ionization energy of the bombarded particle. That is, K.E. (before collision) = K.E. (after collision) + Excitation or Ionisation Energy.

Both the processes of secondary emission and field emission will depend on the work-function of the surface. The higher the work-function the greater would be the field necessary for the emissions. A possible explanation can be advanced, then, if it is assumed that insulating materials have higher work-functions. It would then be expected that the insulated conductors would have higher RIV inception gradients.

The above explanation might be sufficient if corona starts first at the negative half cycle. Possibly this is the case with the bare conductors, because the negative discharges at this half cycle can reinforce the causes of positive corona in the next half cycle increasing the volume of ionization. For the bare conductors the initial discharges were actually observed at the negative peaks.

However, this does not explain the difference in gradient requirements if corona or first burst starts at the positive peak. It is to be noted that for the insulated conductors the pulses were first observed at the positive peaks (See Sec. 4.4).

In the positive half cycle, the electrons formed in the surrounding space by the various ionizing radiations always present, move towards the wire. As the electrons gain energy first excitation of the gas atoms

or molecules will take place due to electron collisions. When the electrons gain more energy they will be able to produce ionization by collision. In the high field region near the conductor, field intensified ionization will take place.

The start of cumulative ionization is associated with the first burst in the case of bare conductors. To initiate the first burst in the case of insulated conductors, some other conditions must be fulfilled. The insulation is acting as a high resistance path in series with the air where slight ionization might have been started. In order to enable the loosely bound charge carriers (inside the dielectric) to migrate and contribute to the conductivity, the insulation resistance must be decreased. Because the insulation is in series with air, the field strength is low in it (see Graph 5.1, page 48). Hence the voltage must be raised to increase the field. It may be required to increase the field up to the point where ionization of the air entrapped in between the conductor and insulation or in small cavities which would always be present inside the dielectrics, starts. This condition is equally applicable for both halves of the cycle. Therefore, in general, a higher gradient may be required for the insulated conductor for

the initiation of corona or radio interference.

It was also found that the RIV inception gradient is a function of radius for both types of conductors. This indicates that not only the maximum gradient, but also the distribution of gradient (which is a function of radius) is important. It is true that corona or RI level is determined by both maximum gradient and gradient distribution in the region of discharge, but the relationship can only be expressed in a very general manner because of the difficulty in determining the exact gradient distribution which critically affects the corona intensity. The p.v.c. covered conductors showed greater RIV immediately after inception. This is possibly because of the different gradient distribution in the two cases. It can be shown from equation (A3.1) and (5.12) that with increasing distance from the conductor surface the gradient falls more rapidly for the bare conductors. This of course, neglects the effect of space charges. The visual corona onset gradients were found to follow the same law (Peek's Law) in both cases. This is possibly because once breakdown at the surface takes place, cumulative ionization can proceed in the surrounding region up to $0.3\sqrt{r}$ which is a required condition for visual corona.

5.3 HIGH FREQUENCY FLUCTUATIONS:[4,1,16]

Negative half cycle:- From the previous section it follows that under sufficiently high surface stress, electrons will be emitted from the conductor by secondary emission or field emission or both. These electrons will be accelerated outward and cause ionization by collision, producing avalanches. But the cumulative effect of the avalanche becomes appreciable only when the electrons produced have traversed several ionizing free paths away from the conductor. This is because for an avalanche of n electrons, $n = 1.e^{\alpha x}$, and thus n will depend on α (Townsend's first coefficient) and also on the distance x. The electric field declines rapidly as the distance increases from the conductor and the electrons in moving away leave behind them relatively immobile positive ions whose space charge reduces the field. Therefore, as the avalanche recedes, the field causing the ionizing electrons weakens. The overall result is the production of a cloud of positive ions whose density rises nearly exponentially from the conductor outward, and then declines more gradually. Retarded by this space charge, the electrons slow down and attach to air molecules to make slow negative ions which eventually drift to the positive cylinder. As

an accompaniment to the ionization a considerable number of atoms are excited by the electrons. With the high fields some molecules are simultaneously ionized and excited. Such excited atoms emit radiations which are capable of ionizing the gas photoelectrically.

The result of positive ion space charge is an immediate increase in the gradient at the conductor surface. This in turn causes an increase in the emission current. This increase in surface gradient continues until the positive ion space charge moves inward to contact the conductor. The surface gradient then drops considerably and ionization stops. As the positive ions move toward the conductor, all their charges are gradually neutralized and during this process the current remains more or less constant. With the clearence of the positive ion space charge, the gradient conditions are restored. So, electron avalanches can occur again.

Mobilities of positive and negative ions differ widely. As a result the period of ionization is very short in comparison with the period of positive ion neutralization at the conductor surface. The periods of ionization are marked by steep pulses in the corona current.

Positive half cycle[33]:- Uhlig explains the causes of pulses from the streamer discharges at the positive half cycle as follows:

When the conductor is positive electrons move at high and increasing velocity toward its surface and disappear there. As the remaining positive ions move away from the conductor at a relatively slow speed, they form a streamer channel. The lines of force are concentrated on the very tip of the streamer, thus causing a sharp voltage drop ahead, and thereby propagating the growth of the discharge path. The density of the ionic cloud travelling in the channel tip cannot surpass certain limits. This is because of the repellent force of the ions. The streamer therefore, spreads and disperses as it travels. This reduces the field stress, which results in a slowing down of channel growth, and finally a temporary standstill. This makes the greatest field stress at a portion of the channel a little further back. The presence of the ionic cloud distorts the field at this point, which causes the channel to branch or continue in a slightly different direction. The whole process repeats and the streamer discharge thus develops in steps. This might explain the causes of the heavily pulsed nature of the current.

5.4 EFFECT OF SPACE CHARGES OF ONE HALF CYCLE ON THE NEXT

The above explanation of the causes of the high frequency fluctuations in each cycle does not account for the effects of the space charges of one half cycle on the next. J.D. Cobine[1] discussed this extensively and also an approximate picture may be seen in "Mechanism of corona from avalanche ionization" as given in Chapter II. Briefly, the space charge produced by corona in one half cycle increases the field strength on the conductor during the first part of the next half cycle. This continues until it is neutralized by ions of opposite sign which are produced around the conductor in the succeeding half cycle. This might be considered as the gross effect. After the neutralization, the individual processes as described earlier may take place.

5.5 PULSES IN INSULATED CONDUCTORS

The processes of high frequency fluctuations described before are strictly for bare conductors. For the insulated conductors, besides these processes which may take place in the air outside the insulation surface, the origin of the pulses may be inside the insulation.

As stated earlier there may be gas-filled voids or holes inside the insulation. The simplest model is to represent a hole by a capacitance C_c in series with a step-pulse generator and with C_b the capacitance of the sound insulation in series with the hole; in parallel will be the capacitance C_a of the remaining insulation. When the void conducts or fires (i.e. ionizes like a gas tube), a current pulse would be obtained due to sudden discharge of C_c. For a void, ionization or deionization will take place at least 4 times in a cycle; hence there would be a minimum of 4 discharges per cycle per individual void.[8]

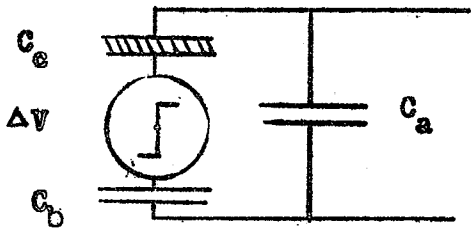

Figure 5.4:- Representation of Ideal Void Inside Insulation.

Moreover, there may be voids of different sizes which would discharge at different values of the voltage wave giving a high number of pulses in each cycle. Whatever may be the causes of the pulses, they will contain high frequency components including that of 1 mc.

5.6 P.V.C. AND POLYETHYLENE COVERED CONDUCTORS COMPARED

1. Power Factor Characteristics:

Up to the critical disruptive voltage the polyethylene covered conductor showed a better power factor characteristic than the p.v.c. covered conductor. Neglecting the ionization effect of the air (which would be very small before the critical voltage), these can be explained from the structure and constituents of the insulations.

Polyvinyl Chloride[9] - It is formed by the polymerization of Vinyl Chloride (CH_2 - CHCl), catalysed by benzoyl peroxide or other oxides. The main constituents of p.v.c. which is used for wire covering are the base polymer (polyvinyl chloride or co-polymer), the plasticizer (tricresyl phosphate, dibutyl phthalate or dioctyl phosphate) to give flexibility, and the stabilizer to combine with any decomposition products formed during the high temperature used for mixing and extrusion, or subsequently in service. Lubricants, dyes, and fillers may also be added. The base polymer has the structure:

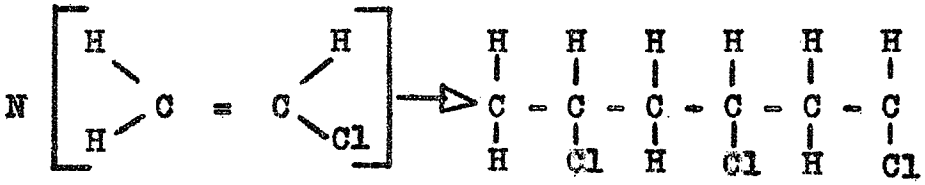

In a two dimensional space, one can represent the molecule as given in Figure 5.5. The bifunctional molecules of vinyl chloride polymerize to form long chains, constituting linear or chain polymers.

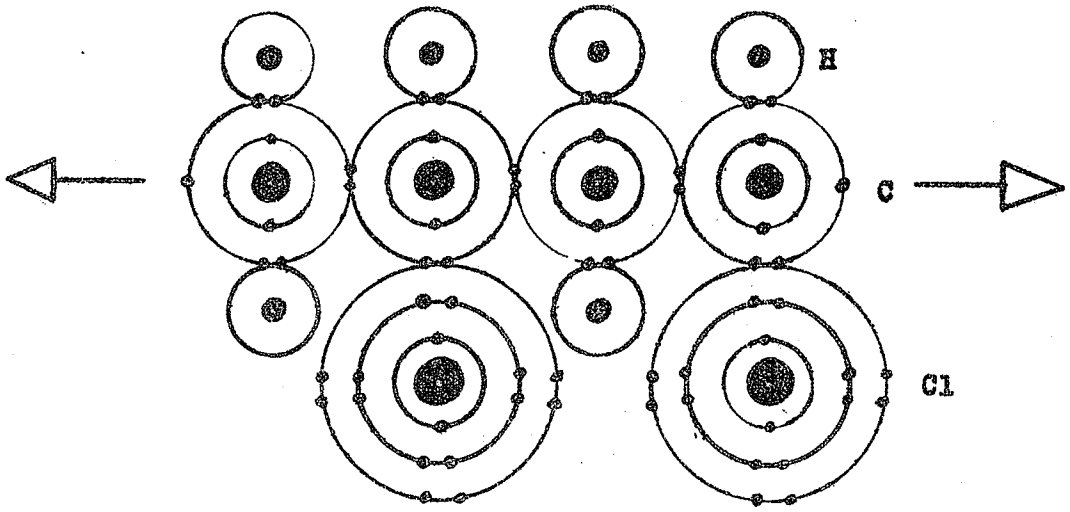

Figure 5.5:- Two Dimensional Representation of Polyvinyl Chloride Molecule.

From the two dimensional representation it is evident that because of the difference in the size of the hydrogen and chlorine atoms the hydrogen end of the molecule is positive and the chlorine end is negative. The polyvinyl chloride molecule is thus polar. Under the action of an a.c. field, therefore, besides other types of polarizations, the dipoles will jump from one equilibrium position to another every cycle to follow the a.c. wave. This dipole orientation from one direc-

tion to another requires energy and is the main cause of high power factor of p.v.c. insulation. In addition the various additives also increase the loss tangent and the dielectric constant which varies from 5 to 6 at 50 cps.

Polyethylene:- It is a chain polymer formed by the polymerization of ethylene gas. The character of the polymer depends on two main factors - the average molecular weight and crystallinity. The electrical properties of polyethylene are practically independent of the grade, being determined by the molecular structure:

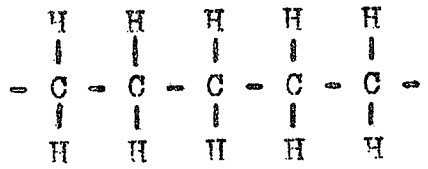

Also it can be represented by:

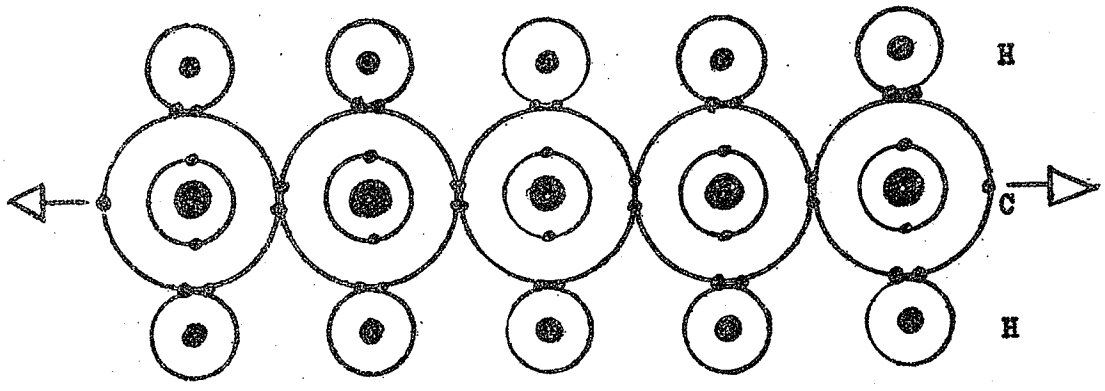

Figure 5.6:- Two Dimensional Representation of Polyethylene Molecule.

From the above representation it can be said that due to the symmetrical configuration the molecule is inherently nonpolar. This characteristic makes the dielectric constant of polyethylene (2.3) smaller than that of p.v.c. Also, though other types of polarizations may be present to some extent, the absence of permanent dipoles should give lower loss tangents for polyethylene than for p.v.c.

This, therefore, explains why better power factor characteristics were obtained for the polyethylene covered conductor.

2. Corona Characteristics:

For the two samples having the same conductor diameter and insulation thickness, the gradient on the insulation surface in air is:

$$\xi_{E_{air}} = \frac{V}{r_i \left[\frac{\ln r_i/r}{K} + \ln R/r_i \right]} \quad \text{.....(From A3.1)}$$

where K is the variable. Therefore, even if the visual corona onset gradient and RIV inception gradient are the same for both types of conductors, the voltage to produce these gradients would be different because of the difference in the dielectric constants. For p.v.c. the value

of K is about 6 and for polyethylene it is 2.3. Hence for p.v.c. covered conductors lower corona onset gradient may be expected and it was actually observed, though the difference was slight.

CHAPTER VI

CONCLUSIONS AND FUTURE STUDIES

6.1 CONCLUSIONS

The following conclusions are drawn from the experimental work described in this thesis.

1. By covering a conductor with some insulation it is possible to operate it at a voltage which is much higher than its critical corona onset voltage. As regards corona the effective conductor radius is increased.

2. The improvement is such that in fact, an insulated conductor shows even better characteristics in some respects than a bare conductor having the same overall diameter.

3. Under the concentric cylinder arrangement, the insulated conductors show better Power Factor Characteristics than the bare ones near the critical voltages, the corona power loss being less for the insulated conductors than for the bare ones having the same overall diameters.

4. The radio noise inception gradient for the insulated conductor is higher than that for a bare conductor having the same overall diameter.

5. For the samples tested the radio noise inception gradients were found to be a function of the overall radii

of the conductors (both insulated and bare).

6. The radio noise inception gradients for both types of wires are slightly lower than those given by Peek's formula for the critical visual corona onset gradients.

7. Though the critical disruptive gradients do not coincide with those obtained from Peek's formula, the visual corona onset gradients for both types of wires conform to it.

8. Even if the visual corona onset gradients are the same for an insulated and a bare conductor having the same overall diameter, because of the effects of insulation, the former will require a higher voltage to produce that gradient.

9. Though the radio noise inception gradients are slightly higher for the insulated conductors, immediately after starting, the magnitudes of their 1 mc. radio influence voltages (Quasi Peak) are considerably higher than those for the bare conductors.

10. Insulated and bare conductors of the same external diameter show approximately equal interference when operated well into the corona region.

11. Polyethylene covered conductors show better Power Factor Characteristics than p.v.c. covered conduc-

tors having the same overall diameters and insulation thicknesses.

12. Since the critical disruptive voltage of an insulated wire is much higher than that of a bare wire having the same conductor diameter, the insulated wire may be operated just below its corona inception voltage without deterioration effects and yet still be at a higher voltage than the inception voltage of the bare wire.

13. The above findings might effectively be used in testing laboratories where radio noise from high voltage is important. However, insulated conductors are probably not feasible on transmission lines primarily because of cost and weather factors.

6.2 FUTURE STUDIES

The investigations regarding the "Effectiveness of insulations in improving corona characteristics" will not be complete unless some other work is done. In fact, this work is just the first step in a big field. First the corona characteristics of #14 bare wire (radius = 0.0815 cm) were found. Its radius was then increased by insulation in one case and copper in the other case. In both cases the increments were made in several steps (finally up to more than twice the radius of #14 wire). For every step experiments were done and a comparative

study was made. During the period of experiments the room temperature and pressure remained more or less constant. Moreover, all the experiments were done at 60 cps a.c. voltage.

Future study could involve variation of more of the parameters, for example,

1. Conductor radius - sizes other than #14 bare might prove interesting.

2. Insulation type - insulations other than P.V.C. and Polyethylene might be explored.

3. Frequency - investigation at higher and lower frequencies and D.C. of both polarities could be undertaken.

4. Surface condition - the effect of dust on the insulation surface could be studied.

5. Temperature and pressure - the effect of temperature and pressure variations might be interesting.

A P P E N D I C E S

APPENDIX I

A1.1 DETERMINATION OF THE DIELECTRIC CONSTANT OF P.V.C.

The sample of the p.v.c. insulated wire was first covered with "Aquadag" and then with lead foil. In a Schering Bridge measurement, the voltage was applied to the conductor and the measuring electrode of the bridge was connected to the lead foil. The ends of the sample were properly guarded. Several measurements were made. Since the normal practice is to measure the dielectric constant at a stress of about 30 V per mil, the value obtained at 1000 V was taken for use. The calculations are shown below.

Length of the sample = 32.5"

Conductor diameter = 0.064"

Overall diameter = 0.126"

Ins. thickness/wall = 0.031"

(Average stress = 1000 V/31 mil = 32.2 V/mil.)

$$C_X = C_S \frac{R_4}{R_3}$$

where, C_S = 103.55 picofarad, R_4 = 2652.5 ohms and R_3 = 730 ohms. Therefore, C_X = 11.58 picofarad per inch.

If C_V is the capacitance per meter with vacuum or air as dielectric, then

$C_V = \frac{2\pi\epsilon_o}{\ln R/r}$; where, R is the overall radius, r is the conductor radius and ϵ_o = 8.84 picofarad per meter.

And

$$K = \frac{C_X}{C_V} = 5.7$$

APPENDIX II

A2.1 DETERMINATION OF VISUAL CORONA FROM TOWNSEND'S THEORY[1,3]

For co-axial cylinders the field at which visual corona starts may be estimated by using Townsend's method. It is assumed that very near the conductor the gap is highly ionized. The film of ionization (cumulative) extends up to a distance r' at which the field strength falls below the critical value of 30 KVP/cm. for air at atmospheric pressure. Though ionization is present at lower fields, 30 KVP/cm. is an approximate value at which cumulative ionization results in breakdown. If E_C is the intensity at the conductor surface and E_0 at the distance r', then

$$\frac{E_0}{E_C} = \frac{r}{r'} \qquad \text{.....(A2.1)}$$

Putting $E_0 = 30$ KVP/cm,

$$r' = \frac{E_C r}{30} \qquad \text{.....(A2.2)}$$

Over the thin film of ionization in the corona envelope the average field may be written as

$$E_{av} = \frac{E_C + 30}{2} \qquad \text{.....(A2.3)}$$

Townsend's formula for breakdown at atmospheric pressure and uniform field is

$$V_S = 30d + 1.35 \qquad \text{.....(A2.4)}$$

d = gap length = energy distance here.

From equation (A2.4)

$$E_S = 30 + \frac{1.35}{d} \quad \text{.....(A2.5)}$$

Equating E_S with average field and putting $d=r'-r$

$$\frac{E_C + 30}{2} = 30 + \frac{1.35}{r'-r} \quad \text{.....(A2.6)}$$

From equations (A2.2) and (A2.6)

$$\frac{E_C + 30}{2} = \frac{1.35}{\frac{E_C r}{30} - r} + 30 \quad \text{.....(A2.8)}$$

which on simplification yields

$$E_C = 30 + \frac{9}{\sqrt{r}} \quad \text{.....(A2.9)}$$

Equations (A2.9) compares favourably with equation (2.3) found by Peek. The distance at which the field drops to the critical value of 30 KVP/cm. is given by equation (A2.9) and (A2.2).

$$r' = r + 0.3\sqrt{r} \quad \text{.....(A2.10)}$$

$$d = r' - r = 0.3\sqrt{r} \quad \text{.....(A2.11)}$$

"This is the distance over which the electric gradient must exceed the dielectric strength of air if corona is to be established."

APPENDIX III

A3.1 DETERMINATION OF GRADIENTS WITH INSULATED WIRES UNDER CONCENTRIC CYLINDER ARRANGEMENTS

In the following concentric arrangement let there be an insulated wire of overall radius r_i and conductor radius r.

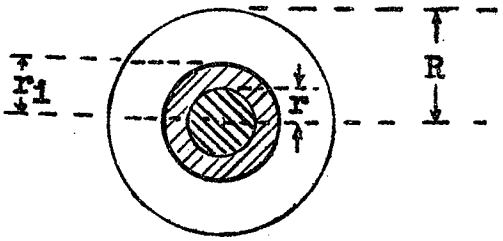

The total capacitance C between the conductor and the cylinder may be taken as the equivalent of two series capacitors C_a with air as dielectric and C_i with the insulation as dielectric. At any distance x from the centre of the wire, the differential permittance,

$$d\left(\frac{1}{C}\right) = \frac{dx}{\epsilon' 2\pi x}$$

where $\epsilon' = \epsilon$, the absolute permittivity of the insulation, or $\epsilon' = \epsilon_o$, the absolute permittivity of air, depending on whether one is considering the element inside the material or in air. On integration,

$$\frac{1}{C} = \frac{1}{C_i} + \frac{1}{C_a} = \frac{1}{2\pi\epsilon}\int_o^{r_i} \frac{dx}{x} + \frac{1}{2\pi\epsilon_o}\int_{r_i}^{R} \frac{dx}{x}$$

$$= \frac{\ln r_i/r}{2\pi\epsilon} + \frac{\ln R/r_i}{2\pi\epsilon_o}$$

From which,

$$C = \frac{2\pi}{\ln \frac{r_i}{r}/\epsilon + \ln R/r_i/\epsilon_o}$$

For an applied voltage V, the flux density at x,

$$D = \frac{CV}{2\pi x}$$

And the field

$$E = \frac{D}{\epsilon'} = \frac{CV}{\epsilon' 2\pi x}$$

It, therefore, follows that

$$E_{air} = \frac{V}{\epsilon_o x \left[\ln \frac{r_i}{r}/\epsilon + \ln \frac{R}{r_i}/\epsilon_o\right]}$$

(x is in air)

Since,

$K = \frac{\epsilon}{\epsilon_o}$ Relative permittivity of the material

$$E_{air} = \frac{V}{x\left[\frac{\ln r_i/r}{K} + \ln \frac{R}{r_i}\right]} \quad \text{.....(A3.1)}$$

Similarly,

$$E_{ins} = \frac{V}{x\left[\ln \frac{r_i}{r} + K \ln \frac{R}{r_i}\right]} \quad \text{.....(A3.2)}$$

(x is inside the insulation)

APPENDIX IV

A4.1 SCHERING BRIDGE TEST DATA

1. Group A - Insulated Samples

TABLE I

Sample 1

Conductor Radius = 0.0815 cm. Ins. Thickness = 0.03805 cm.
Temp. = 21°C. Press. = 73.5 cm. Hg. Air Density Factor = 0.98

Voltage KVP	R_3 Ohms	C_4 tan δ	C_X Picofarad	Remarks
9.2	5500.0	0.0085	50.00	(Too much fluctuation in between 28 and 29.5 KVP)
19.0	5495.0	0.0090	50.0	
26.0	5480.0	0.01	50.01	
28.0				
29.5	5470.1	0.02	50.20	
30.5	5460.0	.075	50.15	
31.5	4500.0	0.205	61.00	(Visual)
36.0	3120.0	0.772	88.00	

TABLE II

Sample 2

Conductor Radius - 0.0815 Ins. Thickness - 0.0584 cm.
Temp. - 21°C. Press. = 73.5 cm. Hg. Air Density Factor = 0.98

Voltage KVP	R_3 Ohms	C_4 tan δ	C_X Picofarad	Remarks
9.2	5344.7	0.00924	51.60	
19.0	5337.7	0.00935	51.62	
29.0	5330.0	0.010	51.65	
31.0	5329.0	0.010	51.66	
31.5				(Fluctuations)
33.0	5320.0	0.040	51.70	
34.5	4883.50	0.2031	56.20	(Visual)

TABLE III

Sample 3

Conductor Radius = 0.0815 cm. Ins. Thickness = 0.0786 cm.
Temp. = 24°C. Press. = 74.4 cm.Hg. Air Density Factor = 0.982

Voltage KVP	R_3 Ohms	C_4 tan δ	C_X Picofarad	Remarks
8.2	5246.0	0.0090	52.40	
18.0	5238.6	0.0092	52.42	
28.0	5224.7	0.0096	52.50	
31.0	5221.2	0.0098	52.55	
33.0	5217.2	0.0100	52.60	
35.0	5210.7	0.0102	52.65	
35.5				(Kick)
36.5	5200.0	0.035	52.70	
37.00	4500.0	0.215	61.00	(Visual)
39.0	3700.0	0.53	74.30	

TABLE IV

Sample 4

Conductor Radius = 0.0815 cm. Ins. Thickness = 0.1182 cm.
Temp. = 23°C. Press. = 74 cm.Hg. Air Density Factor = 0.98

Voltage KVP	R_3 Ohms	C_4 tan δ	C_X Picofarad	Remarks
9.2	5000.0	0.0100	55.00	
19.0	5000.0	0.0101	55.00	
29.0	4998.0	0.0105	55.05	
31.0	4996.0	0.0113	55.08	
33.0	4995.0	0.0115	55.10	
35.0	4990.0	0.0115	55.12	
37.0	4985.0	0.0118	55.15	
39.0				(Kick and Fluc.)
40.5	4980.0	0.050	55.20	
42.0	4021.8	0.2207	68.10	(Visual)
44.0	4020.0	0.3009	68.15	

TABLE V

Sample 5

Conductor Radius. = 0.0815 cm. Ins. Thickness = 0.132 cm.
Temp. =23°C. Press. = 74 cm. Hg. Air Density Factor = 0.98

Voltage KVP	R_3 Ohms	C_4 tanδ	C_X Picofarad	Remarks
9.2	4942.0	0.0101	55.60	
10.0	4935.0	0.0103	55.70	
29.0	4921.5	0.0107	55.80	
34.0	4920.4	0.0110	55.85	
39.0	4915.1	0.0111	55.87	
40.0				(Kick and Fluc.)
42.0	4910.0	0.030	55.90	
44.0	4080.0	0.222	67.30	(Visual)
48.0	4000.0	0.306	69.60	

TABLE VI

Sample 6

Conductor Radius = 0.0815 cm. Ins.Thickness = 0.165 cm.
Temp.= 23°C. Press. = 74. cm.Hg. Air Density Factor = 0.98

Voltage KVP	R_3 Ohms	C_4 tanδ	C_X Picofarad	Remarks
9.2	5000.0	0.0100	55.00	
19.0	4950.0	0.0100	55.00	
29.0	4800.2	0.0110	57.2	
34.0	4800.0	0.0114	57.2	
36.0	4800.0	0.0119	57.2	
39.0	4795.0	0.0119	57.2	
42.0				
44.0	4790.0	0.02	57.3	
45.0	4785.6	0.05	57.35	
48.5	4431.0	0.243	62.4	(Visual)
54.0	3831.0	0.344	71.0	

2. Group B - Bare Conductors.

TABLE VII

Sample 1

#14 Bare Wire. Conductor Radius = 0.0815 cm. Temp. = 21°C.
Press. = 73.5 cm. Hg. Air Density Factor = 0.98.

Voltage KVP	R_3 Ohms	C_4 tan δ	C_X Picofarad	Remarks
9.2	5870.0	0.0084	46.7	
14.0	5860.0	0.0150	46.8	
19.0	5853.0	0.0350	46.85	
22.0	5700.0	0.1803	48.1	
22.5				(Fluctations)
25.0				(Visual)
29.0	4500.0	0.3	61.0	

TABLE VIII

Sample 2

#12 Bare Wire. Radius = 0.1025 cm. Temp. = 20.8°C.
Press. = 73.8 cm. Hg. Air Density Factor = 0.981

Voltage KVP	R_3 Ohms	C_4 tan δ	C_X Picofarad	Remarks
9.2	5600.0	0.0077	49.00	
14.0	5590.0	0.0120	49.10	
19.0	5580.0	0.0210	49.15	
21.0	5560.0	0.0190	49.2	
24.0	5430.0	0.14	50.6	
24.5				
29.0	5000.0	0.5	55.0	(Visual)

TABLE IX

Sample 3
#10 Bare Wire. Radius = 0.1294 cm. Temp. = 20.8°C.
Press. = 73.3 cm. Hg. Air Density Factor = 0.98.

Voltage KVP.	R_3 Ohms	$C_4 \tan\delta$	C_X Picofarad	Remarks
9.2	5343.0	0.0076	51.20	
14.0	5340.0	0.0090	51.25	
19.0	5336.0	0.0098	51.28	
24.0	5300.0	0.0803	51.60	
26.0	5200.0	0.1106	52.50	
28.0				(Too much Fluc.)
31.5				Visual
34.0	4000.0	0.5	68.40	

TABLE X

Sample 4
#8 Bare Wire. Radius = 0.1632 cm. Temp. = 20.8°C.
Press. = 73.3 cm.Hg. Air Density Factor = 0.98

Voltage KVP.	R_3 Ohms	C_4 Tan δ	C_X Picofarad	Remarks
9.2	5100.0	0.0079	53.6	
19.0	5100.0	0.0080	53.6	
29.0	5060.0	0.0150	54.0	
31.0				
34.0	5000.0	0.15	54.6	
37.0	4070.0	0.6	67.0	(Visual)

TABLE XI

Sample 5

#6 Bare Wire. Radius = 0.20575 cm. Temp. = 20.8°C.
Press. = 73.3 cm.Hg. Air Density Factor = 0.98.

Voltage KVP .	R_3 Ohms	C_4 tanδ	C_X Picofarad	Remarks
9.2	4820.0	0.0075	56.70	
19.0	4810.0	0.0078	57.75	
29.0	4800.0	0.0290	56.90	
34.0	4800.0	0.045	56.0	
36.0	4790.0	0.040	56.9	
39.0	4780.0	0.060	57.0	
42.0	4400.0	0.300	62.1	(Visual)

3. Group C - #22 Wires.

TABLE XII

Sample 1

#22 Bare Wire. Diameter = 25.35 mil. Temp. = 23°C
Press. = 74.5 cm. Hg. Air Density Factor = 0.978.

Voltage KVP .	R_3 Ohms	C_4 tanδ	C_X Picofarad	Remarks
4.5	7000.0	0.007	39.15	
9.2	6995.0	0.010	39.20	
11.0	6980.0	0.016	39.22	
12.0	6970.0	0.025	39.35	
13.0	6960.0	0.0742	39.36	
14.0				
15.0	6000.0	0.5	45.80	(Visual)

TABLE XIII

Sample 2
(P.V.C. Insulated #22 Wire). Conductor Diameter = 25.35 mil. Overall Diameter = 43.35 mil. Temp.=23°C. Press.= 74.5 cm.Hg. Air Density Factor = 0.978.

Voltage KVP	R_3 Ohms	C_4 tanδ	C_X Picofarad	Remarks
4.5	6416.0	0.0100	41.00	
9.2	6415.0	0.0112	41.10	
11.0	6414.0	0.0114	41.11	
13.0	6413.0	0.0128	41.12	
15.0	6412.0	0.0144	41.15	
17.0	6410.0	0.020	41.17	
19.0	6400.0	0.035	41.25	
20.0				
22.0	5000.0	0.5	52.80	(Visual)

TABLE IX

Sample 3
(#22 Polyethylene Insulated). Conductor Diameter = 25.35 mil. Overall Diameter = 43.35 mil. Temp. = 23°C. Press.= 74.5 cm. Hg. Air Density Factor = 0.978.

Voltage KVP	R_3 Ohms	C_4 tanδ	C_X Picofarad	Remarks
4.5	6600.0	0.0080	40.00	
9.2	6600.0	0.0105	40.00	
11.0	6595.0	0.0105	40.10	
13.0	6593.0	0.0110	40.10	
15.0	6585.0	0.0116	40.15	
17.0	6580.0	0.0125	40.15	
19.5				
21.5	5000.0	0.05	52.7	
22.5				(Visual)

4. Comparison Of Power Losses*.

TABLE XV

Group A (P.V.C. Insulated)				Group B (Bare)			
Sample 3		Sample 4		Sample 1		Sample 4	
Volts KVP	Power Loss Watts	Volts KVP	Power Loss Watts	Volts KVP	Power Loss Watts	Volts KVP	Power Loss Watts
8.2	0.43	9.2	0.63	9.2	0.45	9.2	0.47
19.0	2.35	19.0	2.70	14.0	1.86	19.0	2.08
28.0	5.70	29.0	6.50	19.0	7.90	29.0	9.16
31.0	6.65	31.0	8.00	22.0	56.6	34.0	127.5
33.0	7.71	33.0	9.25	29.0	207.	37.0	742.
35.0	8.33	35.0	10.40				
37.0	241.	37.0	12.00				
39.0	805.0	42.0	357.				
		44.0	532.				

* For each sample power losses are calculated for a length of 1000 ft.

5. Visual Critical Corona Voltages and Gradients.

TABLE XVI

Group A - Insulated Conductors						
Samples	Radius cm. (r_i)	Ins. Thickness/ Wall cm.	E_c Calculated. (m=1) KVP/cm	V_c Calculated (m=1) KVP	V_c Measured KVP	Value of m.
1	0.1195	0.0380	57.6	33.0	31.50	0.955
2	0.1399	0.0584	55.5	36.2	34.5	0.954
3	0.1601	0.0786	53.8	39.1	37.0	0.947
4	0.1997	0.1182	51.5	44.7	42.0	0.940
5	0.2135	0.1320	50.7	46.6	44.0	0.953
6	0.2465	0.1650	49.3	50.6	48.5	0.957

TABLE XVII

Group B - Bare Conductors						
Samples	Radius cm. (r_i)	Increase In Radius From 0.0815 cm.	E_c Calculated. (m=1) KVP/cm.	V_c Calculated. (m=1) KVP.	V_c Measured KVP.	Value of m.
1	0.0815	0.0000	63.5	26.25	25.0	0.953
2	0.1025	0.0210	60.0	30.10	28.5	0.950
3	0.1294	0.0479	57.7	34.0	31.5	0.930
4	0.1632	0.0817	53.7	38.0	37.0	0.958
5	0.2057	0.1242	51.1	43.0	42.0	0.952

A4.2 RIV TEST DATA

TABLE XVIII

Group A - Insulated Conductors

Temperature 21°C. Pressure 74.5 cm. Hg.

Sample 1		Sample 2		Sample 3		Sample 4		Sample 5	
Volts KVP	RIV μV	Volts KVP	RIV μV	Volts KVP	RIV μV	Volts KVP	RIV μV	Volts KVP	RIV μV
0	2.5	0	2.5	0	2.5	0	2.5	0	2.5
10	2.5	10	2.5	10	2.5	10	2.5	10	2.5
20	2.5	20	2.5	20	2.5	20	2.5	20	2.5
28	2.5	30	2.5	30	2.5	30	2.5	30	2.5
29	10	31.5	2.5	35	2.5	35	2.5	40	2.5
30	60	33	20	35.5	10	39	2.5	42	20
32	100	34	100	36	30	40	10	43	30
35	80	36	120	37.5	80	41	20	45	160
37	60	38	150	39	100	42	100	46.5	190
39	60	40	150	41	120	43	130	51	180
41	60	42	100	44	100	44	150	54	160
44	70	44	85	47	90	45	160		
47	80	46	80	49	90	46	170		
49	100	49	80			47	170		
						49	160		
						51	130		
						54	100		

TABLE XIX

Group B - Bare Conductors

Sample 1		Sample 2		Sample 3		Sample 4	
Volts KVP	RIV μV	Volts KVP	RIV μV	Volts KVP	RIV μV	Volts KVP	RIV μV
0	2.5	0	2.5	0	2.5	0	2.5
10	2.5	10	2.5	10	2.5	10	2.5
20	2.5	20	2.5	20	2.5	20	2.5
21	2.5	23	2.5	25	2.5	30	2.5
22	7	24	7	28	2.5	31	2.5
24	13	26	15	28.5	7	32	3
26	20	28	25	30	20	34	7.5
28	25	30	28	32	30	36	11
30	30	32	35	34	35	38	18
32	35	34	42	36	40	40	20
34	40	36	48	38	45	42	25
36	45	38	55	40	50	44	35
38	45	40	60	42	55	46	40
40	50	42	70	44	65	48	45
42	60	46	80	49	80	50	50
44	65						
46	65						
50	70						

BIBLIOGRAPHY

A. BOOKS

1. J.D. Cobine, Gaseous Conductors. McGraw-Hill Book Company, Inc., 1941, pp.252-89.

2. F.W.Peek, Jr., Dielectric Phenomena In High Voltage Engineering, McGraw-Hill Book Company, Inc., 1929.

3. S. Whitehead, Dielectric Phenomena. New York: D. Van Nostrand Company Inc., pp.93-160.

4. L.B. Loeb, Fundamental Processes Of Electrical Discharge In Gases. New York: John Wiley & Sons, Inc., 1939, pp.485-520.

5. J.L. Martin, Jr., Physical Basis For Electrical Engineering. Englewood Cliffs. N.J.,: Prentice-Hall, Inc., 1957.

6. A.J. Dekker, Electrical Engineering Materials. Englewood Cliffs, N.J.:Prentice-Hall, Inc., 1959.

7. J.B.Whitehead, Lectures On Dielectric Theory And Insulation. McGraw-Hill Book Company, Inc., 1927. pp.7-16 and 118-140.

8. Jackson, The Insulation Of Electrical Equipment, John Wiley & Sons, Inc.

9. J.B. Birks, Modern Dielectric Materials. London: Heywood & Company, Ltd., 1960, pp.9-23 and 95-111.

10. H.H.Skilling, Fundamentals Of Electric Waves. New York: John Wiley & Sons, Inc., 1948, pp.59-60.

11. A.R. Von Hippel, Dielectric Materials And Applications. The Technology Press Of M.I.T. And John Wiley & Sons, Inc., 1954.

12. A.R. Von Hippel, Dielectrics And Waves. New York: John Wiley & Sons, Inc., 1954

13. E.W. Golding, Electrical Measurements And Measuring Instruments. London: Sir Isaac Pitman & Sons, Ltd., 1959, pp.159-57.

14. B. Hague, Alternating Current Bridge Methods. London: Sir Isaac Pitman & Sons, Ltd., 1957, pp. 350-70.

15. C.P. Smyth, Dielectric Behaviour and Structure, McGraw-Hill Book Company, Inc., 1955, pp.181-84 and 186-87.

B. TECHNICAL PAPERS

16. G.R. Slemon, Radio Influence From High Voltage Corona. AIEE Transactions, Vol. 68, Pt. I. 1949, pp. 198-204.

17. A.S. Denholm, The Pulses And Influence Voltage Of Power Frequency Corona. Power Apparatus And Systems, October 1960, pp. 698-707.

18. T.W. Liao, W.A. Keen, Jr., D.R. Powell, Relationship Between Corona And Radio Influence On Transmission Lines, Laboratory Studies, I-Point And Conductor Corona. AIEE Transactions, Pt.III, (Power Apparatus And Systems), Vol. 76, August 1957, pp.530-40 .

19. G.W. Trichel, The Mechanism Of The Negative Point-To-Plane Corona Near Onset. Physical Review, New York, N.Y., Vol. 54, 1938, pp.1078-84.

20. G.W. Trichel, The Mechanism Of The Positive Point-To-Plane Corona In Air At Atmospheric Pressure. Ibid., Vol. 55, 1939, pp.382-90.

21. L.B. Loeb, The Mechanism Of The Trichel Pulses Of Short Time Duration In Air, Ibid., Vol. 86, 1952, p.256.

22. L.B. Loeb, W. Leigh, Positive Needle Point Corona Studies At Atmospheric Pressure. Ibid., Vol. 51, 1937, p.149.

23. C.G. Miller, L.B.Loeb, Positive Co-axial Cylindrical Corona Discharge In Pure N_2O_2 And Mixtures Thereof. Journal Of Applied Physics, Vol.22, 1951, pp.492-503.

24. M.R. Amin, Fast Time Analysis Of Intermittent Point-To-Plane Corona In Air.III - The Negative Point Trichel Pulse Corona. Ibid., Vol. 25. 1954, p.627.

25. M.R. Amin, Fast Time Analysis Of Intermittent Point-To-Plane Corona In Air. I - Positive Point Burst Pulse Corona. Ibid., p.210.

26. M.R. Amin, Fast Time Analysis Of Intermittent Point-To-Plane Corona In Air. II - Positive Pre-Onset Streamer Corona. Ibid., p.358.

27. T.W. Liao, Corona Type Noise And Its Measurements. NRC, Canada, High Voltage Symposium Paper, 1956.

28. A.S. Denholm, Radio Noise Testing Of High Voltage Line Equipment. NRC, Canada, High Voltage Symposium Paper, 1956.

29. M.C. Perz, Characteristics Of Corona Noise. Ontario Hydro Research News, October-December 1960.

30. O. Nigol, The Corona Loss Problem. Ontario Hydro Research News, January-March, 1959.

31. G.K. Lambert, Factors Influencing The Corona Inception Voltage Extra High Voltage Lines, NRC, Canada, High Voltage Symposium Paper, 1956.

32. C.A.E. Uhlig, A.C. Corona Current And Losses On Thin Wires From Onset To Sparkover. NRC Canada, High Voltage Symposium Paper, 1956.

33. C.A.E. Uhlig, The Ultra Corona Discharge, A New Discharge Phenomenon Occurring On Thin Wires. NRC, Canada, High Voltage Symposium Paper, 1956.

34. D.E. Jones, Radio Interference Studies On Woodpole Transmission Lines Operated At 250 Kv. Ontario Hydro Research News, July-September, 1957.

35. D.E.Jones, And J.R. Leslie, Radio Interference Problems At Extra High Voltage. Ontario Hydro Research News, January-March, 1959.

36. O. Nigol And J.G. Cassan, Corona Loss Research At The Coldwater Project. Ontario Hydro Research News, January-March, 1961.

37. J. Reichman And J.R. Leslie, Radio Interference Studies At The Coldwater Project. Ont. Hydro Research News, January-March 1961.

38. Kino, Nagaya, Takaoka, Corona Noise Tests On Extra High Voltage Lines With The Enclosed Type Concentric Cylinder. Electro-Technical Journal, Japan, 1958.

39. C.J. Miller, Jr. Mathematical Prediction Of Radio And Corona Characteristics Of Smooth Bundled Conductors, AIEE Transactions, Pt.III, 1956, p.1029.